Cortical Composition Hierarchy Driven by Spine Proportion Economical Maximization or Wire Volume Minimization

Jan Karbowski*

Institute of Applied Mathematics and Mechanics, University of Warsaw, Warsaw, Poland

* jkarbowski@mimuw.edu.pl

Abstract

The structure and quantitative composition of the cerebral cortex are interrelated with its computational capacity. Empirical data analyzed here indicate a certain hierarchy in local cortical composition. Specifically, neural wire, i.e., axons and dendrites take each about 1/3 of cortical space, spines and glia/astrocytes occupy each about $(1/3)^2$, and capillaries around $(1/3)^4$. Moreover, data analysis across species reveals that these fractions are roughly brain size independent, which suggests that they could be in some sense optimal and thus important for brain function. Is there any principle that sets them in this invariant way? This study first builds a model of local circuit in which neural wire, spines, astrocytes, and capillaries are mutually coupled elements and are treated within a single mathematical framework. Next, various forms of wire minimization rule (wire length, surface area, volume, or conduction delays) are analyzed, of which, only minimization of wire volume provides realistic results that are very close to the empirical cortical fractions. As an alternative, a new principle called "spine economy maximization" is proposed and investigated, which is associated with maximization of spine proportion in the cortex per spine size that yields equally good but more robust results. Additionally, a combination of wire cost and spine economy notions is considered as a meta-principle, and it is found that this proposition gives only marginally better results than either pure wire volume minimization or pure spine economy maximization, but only if spine economy component dominates. However, such a combined meta-principle yields much better results than the constraints related solely to minimization of wire length, wire surface area, and conduction delays. Interestingly, the type of spine size distribution also plays a role, and better agreement with the data is achieved for distributions with long tails. In sum, these results suggest that for the efficiency of local circuits wire volume may be more primary variable than wire length or temporal delays, and moreover, the new spine economy principle may be important for brain evolutionary design in a broader context.

Author Summary

Cerebral cortex is an outer layer of the brain in mammals, and it plays a critical part in various cognitive processes such as learning, memory, attention, language, and consciousness. The cerebral cortex contains a number of neuroanatomical parameters whose values are essentially conserved across species and brain sizes, which suggests that these particular parameters are somehow important for brain efficient functioning. This study shows that the fractional volumes of five major cortical components both neuronal and non-neuronal (axons, dendrites, spines, glia/astrocytes, capillaries) are also approximately conserved across mammals, and neural wire (axons and dendrites) occupies the most of cortical space. Moreover, the fractional volumes form a special hierarchy of dependencies, being approximately equal to integer powers of 1/3. Is there any evolutionary principle of cortical organization that would explain these properties? This study finds that there are two different theoretical principles that can provide answers: one standard related to minimization of neural wire fractional volume, and a new proposition associated with economical maximization of spine content. However, the latter principle produces more robust results, which suggests that spine economical maximization is potentially an alternative to the more common "wire minimization" in explaining the cortical layout. Therefore, the current study can become an important contribution to our understanding (or debating) of the main factors influencing the evolution of local cortical circuits in the brain.

Introduction

The gray matter of cerebral cortex is composed primarily of neurons with their extended axonal and dendritic processes, synapses (mostly dendritic spines) connecting different neurons, non-neuronal cells called glia (of which astrocytes are likely the most important), and microvasculature (capillaries). It is thought that neurons and synapses are the main computational and functional elements, whereas glia and capillaries serve supporting or modulatory roles associated with supplying metabolic substrates (oxygen and glucose) to neurons and synapses based on their demands [1, 2]. The experimental data show that there are certain scaling regularities in the arrangement of neuronal, synaptic [3–5], and capillary [6] processes. It is commonly hypothesized that these scaling rules may be the consequence of the design principle called neural "wiring minimization" or "wiring economy" [3, 7–10], or efficiency in functionality-cost trade-offs [11–14]. However, there are some indications that wiring length minimization is not enough to explain the pattern of global connections in the macaque cortex and in the nematode *C. elegans* nervous system [15, 16], and even small-scale networks of macaque and cat visual cortices perform sub-optimally in terms of wire length reduction [17]. This opens a possibility for some other optimization principles governing brain architecture.

Here, it is proposed a new, alternative, design principle that can be called "spine economical maximization" or spine economy. It is based on maximization of spine proportion in the cortex with simultaneous penalization of spine size. This scenario is equivalent to requiring that in a given cortical volume there are as many information storing connections between neurons as possible (maximal functionality) that cost as little energy as possible (economical approach, for bigger spines use more energy). Moreover, we require that these connections are efficiently coupled with astrocytes and capillaries, and the whole system of neuronal and non-neuronal elements is treated within a single theoretical framework. The choice of the guiding principle associated with spine economy is motivated by the following empirical results: (i) Axo-spinal synaptic connections are the most numerous in the cortical gray matter [18] and are very

important not only for short-term neuronal communication [12], but also for long-term information storage [19]; (ii) Mammalian brain is metabolically expensive [20–22], which means that energy is an important constraint on brain function [14, 23, 24]; (iii) Spines are likely the major users of metabolic energy in the cortical gray matter [25–27], as is reflected in a strong correlation between cortical synaptogenesis and its energetics [27, 28], which suggests that spine number or size can be limited by available energy.

The new hypothetical principle associated with spine economy is tested here for local organization of cortical circuits. Specifically, it is tested if fractional occupancy of space by the main cortical components predicted on a basis of the spine economical maximization principle agrees with empirical data. Fractional distribution of volume taken by neuronal and non-neuronal elements should be an important aspect of local cortical organization, because densities of neurons, glia, and vasculature are mutually correlated across cortical regions and layers [29–31]. Thus, too much space taken by one component can lead, due to competition, to underperformance of other components [32] or to an excessive cortical size [33], both of which can be undesirable for brain efficient design and functionality. Thus, some neuroanatomical balance between fractional volumes of cortical elements seems necessary. Unfortunately, it is virtually not known whether these fractions are variable or preserved across species. This interesting topic was only briefly addressed before, with the suggestion that the combined fraction of neuronal wire (axons and dendrites) can result from minimization of temporal delays in inter-neuronal signaling [8]. However, from an evolutionary perspective, the knowledge of fractional distribution of all major cortical components, also those supplying metabolic energy, should add an important information to our understanding of the geometric layout of the cortex and for testing various hypotheses concerning its design principles [34].

The paper is organized as follows. First, empirical data on fractional volumes of cortical components are analyzed. In particular, we look for regularities in the data within and across species. We build and study a theoretical model of cortical composition with coupled neuronal and non-neuronal elements. Next, we investigate which optimization principle can best explain the empirical facts. Three classes of optimization models are considered. One is based on a standard principle of neural wire minimization and includes minimization of wire length, wire surface area, wire volume, and local temporal delays. Second class is based on a new proposition of spine economical maximization. Third class is a linear combination of the first two types of models, i.e., it mixes wire cost with spine economy. All kinds of models are based on an implicit assumption that evolution had optimized the nervous system according to some rules [13, 14, 35–37].

Results

Empirical composition of the cerebral cortex across mammals reveals hierarchical organization

Existing experimental data on fractional volumes of cortical gray matter components were analyzed (see the Methods), and it is found that these fractions exhibit a certain hierarchy, since they can be approximated by integer powers of 1/3 (Table 1; Fig 1). Specifically, axons and dendrites occupy each about 1/3 of cortical space, dendritic spines and glia/astrocytes constitute each roughly $(1/3)^2$ of the cortex, and capillaries take an extremely small volume fraction around $(1/3)^4$ (Table 1; Fig 1). This regularity is called here the rule of "powers of 1/3". Moreover, an allometric analysis reveals that the fractions of all examined cortical components are species- and brain size independent, i.e. they do not correlate significantly with cortical size and scale with exponents close to zero (Table 1; Fig 2). Typical values for axons: exponent = −0.036, $R^2 = 0.083$, $p = 0.713$; for dendrites: exponent = −0.002, $R^2 = 0.037$, $p = 0.717$; for

Table 1. Structural composition of the gray matter of cerebral cortex.

| Species	Volume fraction (%)				
	Axons	**Dendrites**	**Spines**	**Glia/Astrocytes**	**Capillaries**
Mouse	34.0	35.0	14.0	11.0*	0.7 ± 0.1
Rat	47.0 ± 5.0	35.0 ± 5.0	9.0	8.0 ± 4.0*	1.4
Rabbit	47.0 ± 5.5	34.7 ± 3.9	5.7 ± 0.8	12.7 ± 2.2*	–
Cat	27.8 ± 5.7	31.0 ± 6.3	–	15.5	2.1 ± 0.5
Macaque	–	33.0 ± 19.0	4.5 ± 0.8	–	0.9 ± 0.1
Human	–	35.4 ± 23.7	14.8 ± 9.9	11.5 ± 3.4	1.7 ± 0.3
Species mean	39.0 ± 2.3	34.0 ± 5.3	9.6 ± 2.0	11.7 ± 1.1	1.4 ± 0.1
Normalized mean	40.8 ± 2.4	35.5 ± 5.5	10.0 ± 2.1	12.2 ± 1.2	1.5 ± 0.1
Rule "powers of 1/3"	33.3	33.3	11.1	11.1	1.2

Symbol * corresponds to the fraction of unspecified glia cells. The next-to-last line contains normalized to 100% mean fractional values over species. The last line is a theoretical prediction based on a "powers of 1/3" rule. References for the data are given in the Methods.

doi:10.1371/journal.pcbi.1004532.t001
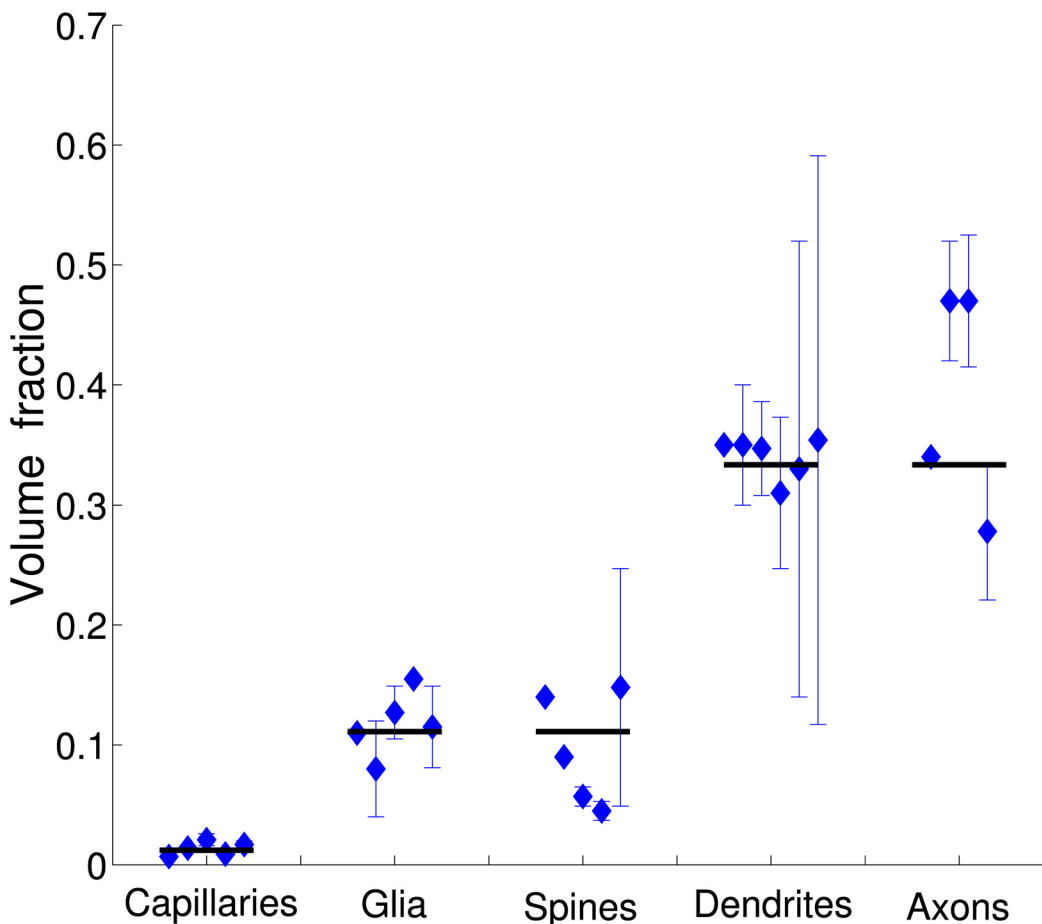
Fig 1. Hierarchical organization of the five major components in the gray matter of cerebral cortex. Empirical data points for each component are denoted by blue diamonds and correspond to different mammals (see Table 1). Solid black lines represent integer powers of the fraction 1/3. In particular, these fractions are: $(1/3)^4$ for capillaries, $(1/3)^2$ for glia and spines, and $1/3$ for dendrites and axons. Note, that on average empirical fractional volumes across species approximately conform to this simple rule.

doi:10.1371/journal.pcbi.1004532.g001
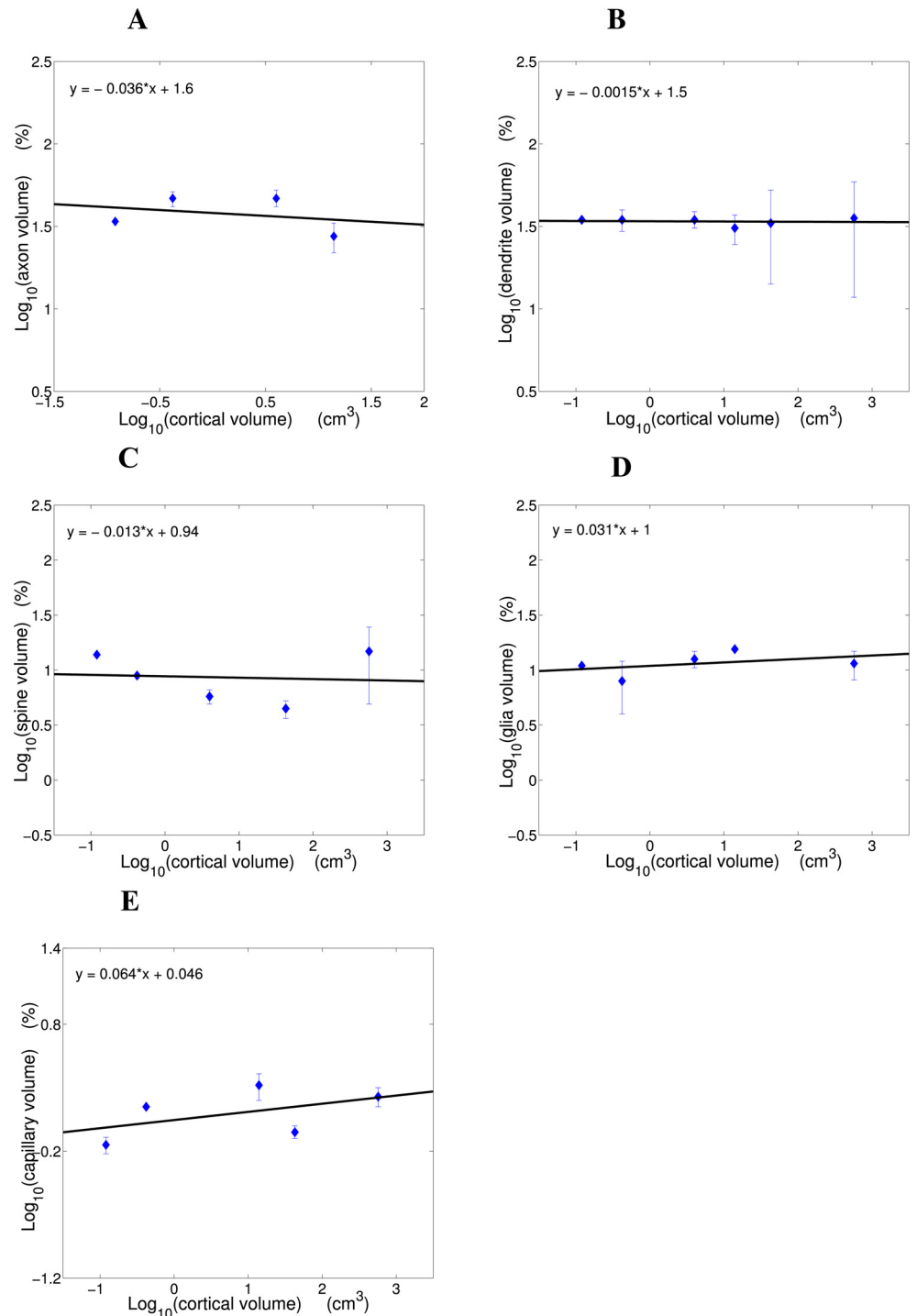
Fig 2. Scaling dependence of fractional volumes of the basic cortical components on cortical gray matter volume. (A) Axon fractional volume, (B) dendrite fractional volume, (C) spine fractional volume, (D) glia fractional volume, and (E) capillary fractional volume as functions of cortical volume in log-log coordinates. Note a conservation trend across mammals. Scaling plots were constructed based on data in Table 1. The following volumes of cortical gray matter (two hemispheres) were used: mouse 0.12 cm^3 [38], rat 0.42 cm^3 [39], rabbit 4.0 cm^3 [40], cat 14.0 cm^3 [40], macaque monkey 42.9 cm^3 [39], human 571.8 cm^3 [39].

doi:10.1371/journal.pcbi.1004532.g002

spines: exponent = −0.013, R^2 = 0.008, p = 0.885; for glia/astrocytes: exponent = 0.031, R^2 = 0.180, p = 0.477; and for capillaries: exponent = 0.064, R^2 = 0.243, p = 0.399 (Fig 2).

Optimality principles for local cortical circuits

It is possible that the relative constancy of the fractional occupancy of cortical space and its simple hierarchy reflect some kind of evolutionary optimized principle. Three such principles are considered: one associated with neural wire minimization, second with spine proportion economical maximization, and the third proposition is the mixture of the first two. The last choice means that we consider the possibility of some "meta-principle", which includes the contributions of both primary principles (wire minimization and spine economy maximization) with some weights related to their importance. The most general fitness function F, or benefit-cost function, associated with such a meta-principle, which we want to minimize, is given by (see the Methods, in particular the section "The fitness functions" for the derivation)

$$F = f \frac{(rx + y)}{\bar{u}^{\gamma_1}} - (1 - f) \frac{s}{\bar{u}^{\gamma_2}} + \lambda (x + y + s + g + c - 1), \tag{1}$$

where x, y, s, g, c are respectively volume fractions of axons, dendrites, spines, glia, and capillaries in the cortical gray matter, and λ is the Lagrange multiplier associated with a mathematical constraint of the fractions normalization. The symbol f is the control parameter ($0 \leq f \leq 1$), or mixing ratio, measuring a relative contribution (importance) to the fitness function of the two contrasting notions: wire minimization and spine economical maximization. If $f = 1$ then the function F corresponds to wire cost only, whereas if $f = 0$ then the function F describes spine economy only (the negative sign in front of $(1 - f)$ is necessary to obtain maximum for spine content). The symbol $\bar{u}$ is the average spine volume, r is some positive measure of asymmetry between axons and dendrites, γ_1 and γ_2 are positive exponents. Different values of γ_1 correspond to different kinds of wire minimization. In particular, $\gamma_1 = 0$ relates to wire volume minimization, $\gamma_1 = 1/3$ corresponds to wire surface area minimization, $\gamma_1 = 2/3$ is associated with wire length minimization, and $\gamma_1 = 5/6$ relates to local temporal delays minimization (see the Methods). The parameters r, γ_2, and f constitute the free parameters.

In the next sections we study theoretical consequences of minimization of the fitness function represented by Eq (1). Specifically, we find optimal values of fractional volumes of the cortical components and compare them with the empirical data.

Optimal fractional volumes of cortical components: Wire minimization vs. spine economical maximization

Wire minimization principle corresponds to $f = 1$ in Eq (1). For this scenario the optimal fractional volumes of cortical components depend on two parameters: γ_1 and r. The dependence of optimal fractions on γ_1 is critical. If $\gamma_1 = 0$ (the case of wire fractional volume minimization) then the theoretical fractions can be similar to the empirical values in Table 1 (the next-to-last line) only when $r \sim 1$ (Fig 3). If $\gamma_1 > 0$ (the other types of wire minimization), regardless of the value of r, the optimal fractions of glia/astrocytes and capillaries vanish, which is unrealistic (Fig 3A and 3C). Moreover, only the case $\gamma_1 = 0$ produces finite reliable values of the average spine volume $\bar{u}$ (Table 2); for $\gamma_1 > 0$ we obtain $\bar{u} \mapsto \infty$. The abrupt transition in solutions from $\gamma_1 = 0$ to $\gamma_1 > 0$ is reminiscent of discontinuous phase transitions. The dependence of the optimal fractional volumes on r is more smooth (if $\gamma_1 = 0$; Fig 3B and 3D). Realistic fractions are obtained for almost symmetrical situation, i.e. when r is close to 1; too small or too large r produces vanishing fractions of either dendrites or axons (Fig 3B and 3D). Moreover, all the
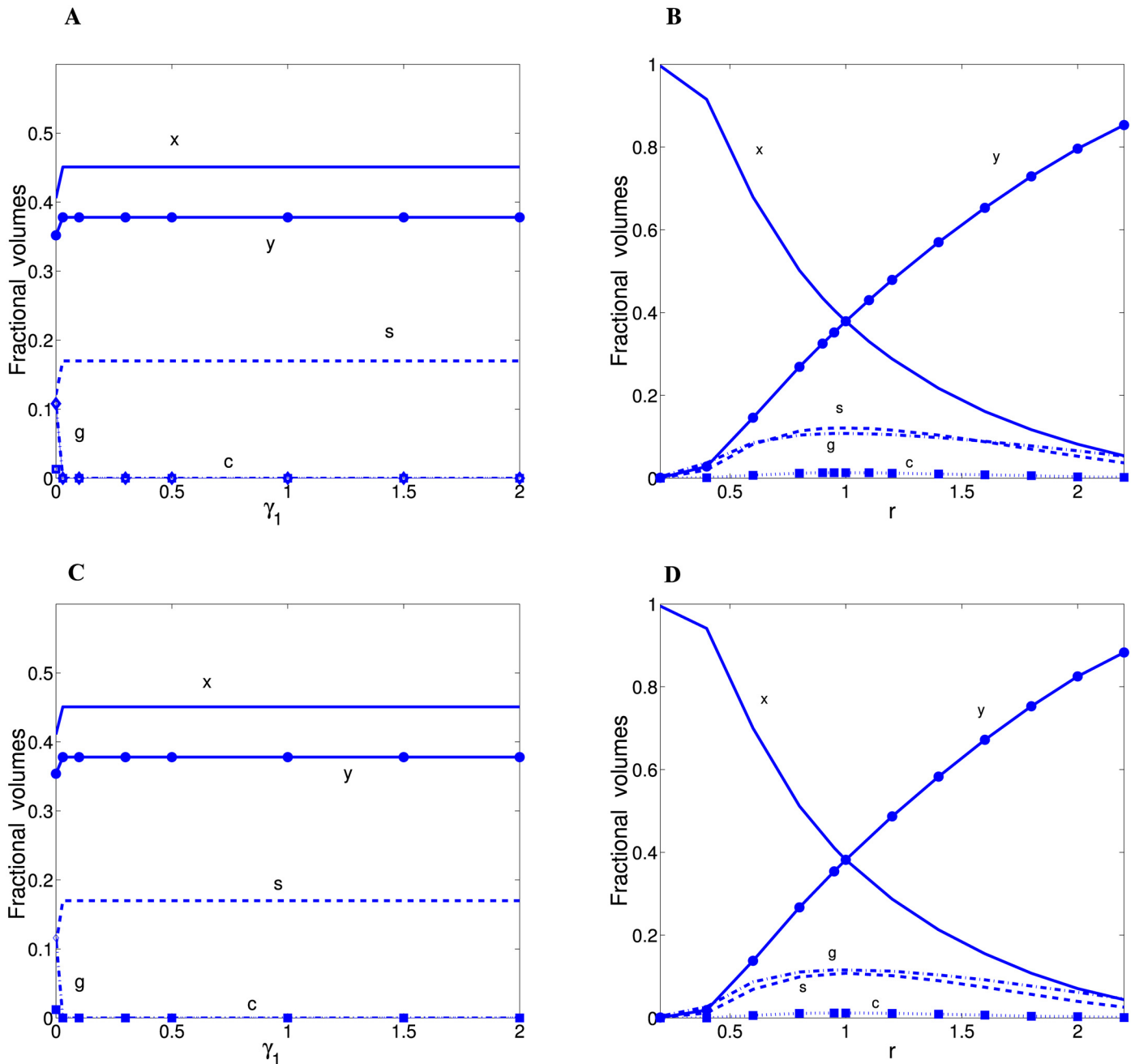
Fig 3. Optimal fractional volumes for neural "wire minimization" principle as functions of the exponent γ_1 and r. The results for short-tailed Gamma ($n = 2$) distribution are in (A) and (B), and for long-tailed Log-normal distribution in (C) and (D). Note that for $\gamma_1 > 0$ (panels A and C) all fractions are constant, in particular glia/astrocytes and capillaries vanish ($g = c = 0$). Parameter values: for panels (A) and (C) $r = 0.95$, while for panels (B) and (D) $\gamma_1 = 0$. Additionally, for log-normal $\sigma = 0.3$. For all panels $\theta = 0.321 \ \mu m^3$.

doi:10.1371/journal.pcbi.1004532.g003

described results look qualitatively similar regardless of the asymptotic nature of the distributions of spine sizes (compare Fig 3A and 3B vs. Fig 3C and 3D).

Alternatively, for spine economical maximization principle, i.e. for $f = 0$ in Eq (1), the optimal fractions of cortical components depend moderately on the exponent γ_2. This dependence is displayed in Fig 4 for four distributions of spine sizes: two with short tails (Gamma

Table 2. The best optimal theoretical fractional volumes and related parameters in the cortex for a particular case of "wire minimization" principle associated with wire volume minimization ($\gamma_1 = 0$). The optimal fractions correspond either to minimal Euclidean distance (ED) or minimal Mahalanobis distance (MD) between theory and data (given in bold face).

Spine size distribution	θ	Optimal parameters								ED	MD
		x	y	s	g	c	$\bar{u}$	P	r		
Exponential	0.100	0.388	0.330	0.068	0.201	0.014	0.157	0.528	0.94	**0.091**	6.981
	0.100	0.403	0.316	0.067	0.200	0.013	0.157	0.528	0.91	0.094	**6.942**
	0.321	0.423	0.371	0.111	0.085	0.009	0.935	0.709	0.96	**0.045**	6.485
	0.321	0.397	0.397	0.112	0.085	0.010	0.936	0.710	1.00	0.058	**6.360**
Gamma (n = 1)	0.100	0.376	0.316	0.081	0.210	0.017	0.175	0.684	0.93	**0.104**	7.842
	0.100	0.442	0.259	0.078	0.206	0.016	0.175	0.682	0.80	0.134	**7.427**
	0.321	0.413	0.357	0.119	0.099	0.012	0.793	0.805	0.95	**0.030**	3.991
	0.321	0.396	0.374	0.119	0.099	0.012	0.794	0.806	0.98	0.037	**3.892**
Gamma (n = 2)	0.100	0.366	0.310	0.086	0.219	0.019	0.175	0.753	0.93	**0.115**	9.078
	0.100	0.463	0.230	0.080	0.210	0.017	0.174	0.750	0.74	0.163	**8.173**
	0.321	0.406	0.352	0.121	0.108	0.013	0.715	0.846	0.95	**0.026**	2.681
	0.321	0.395	0.363	0.121	0.108	0.013	0.715	0.846	0.97	0.030	**2.640**
Rayleigh	0.100	0.368	0.305	0.082	0.226	0.019	0.159	0.734	0.92	**0.124**	9.623
	0.100	0.471	0.221	0.076	0.216	0.016	0.158	0.731	0.72	0.177	**8.701**
	0.321	0.405	0.352	0.117	0.113	0.013	0.642	0.822	0.95	**0.020**	2.271
	0.321	0.394	0.362	0.117	0.113	0.013	0.642	0.822	0.97	0.025	**2.236**
Log-logistic	0.100	0.404	0.350	0.097	0.136	0.013	0.404	0.683	0.95	**0.015**	2.378
	0.100	0.399	0.356	0.097	0.136	0.013	0.404	0.684	0.96	0.017	**2.351**
	0.321	0.399	0.348	0.124	0.114	0.014	0.671	0.891	0.95	**0.027**	1.803
	0.321	0.403	0.334	0.123	0.124	0.015	0.584	0.910	0.93	0.031	**1.448**
Log-normal	0.100	0.418	0.367	0.072	0.133	0.010	0.311	0.472	0.96	**0.034**	5.734
	0.100	0.401	0.356	0.073	0.158	0.012	0.244	0.513	0.96	0.045	**4.801**
	0.321	0.411	0.354	0.106	0.116	0.012	0.561	0.731	0.95	**0.010**	2.897
	0.321	0.402	0.341	0.110	0.133	0.015	0.475	0.804	0.94	0.021	**1.405**

For log-logistic distribution the minimal ED and MD were obtained for the parameter $\beta = 1.5$ if $\theta = 0.100$, and if $\theta = 0.321$ then $\beta = 3.5$ for minimal ED and $\beta = 4.5$ for minimal MD. For log-normal distribution the minimal ED was reached for $\sigma = 0.7$ and minimal MD for $\sigma = 0.55$ if $\theta = 0.100$, and if $\theta = 0.321$ then $\sigma = 0.3$ for minimal ED and $\sigma = 0.2$ for minimal MD.

and Exponential distributions) and two with long tails (Log-logistic and Log-normal). As can be seen the optimal fractions of axons and dendrites are equal and about 0.4, and they are qualitatively almost independent of γ_2 and spine size distribution. Similarly, the capillary content is relatively stable at about 0.01 or a little less (Fig 4). In contrast, the fractions of spines and astrocytes/glia can change significantly as a function of γ_2. Typically, the spine proportion decreases with increasing γ_2, whereas glia/astrocytes content depends non-monotonically on γ_2, but both of them are restricted from above (spines by ~ 0.16 and astrocytes by ~ 0.14). These trends are preserved as we change the distributions of spine volumes from short-range to long-range (Fig 4A and 4B vs. Fig 4C and 4D). The pattern for the remaining two distributions (Gamma n = 1 and Rayleigh; not shown) is very similar. Overall, the optimal fractions of cortical components can either vary with γ_2 or not, but these dependencies are essentially invariant with respect to the distribution type of spine sizes. More importantly, the optimal fractional volumes are quantitatively similar to the empirical values given in Table 1 (the next-to-last line) for a broad range of γ_2.

A

B

C

D
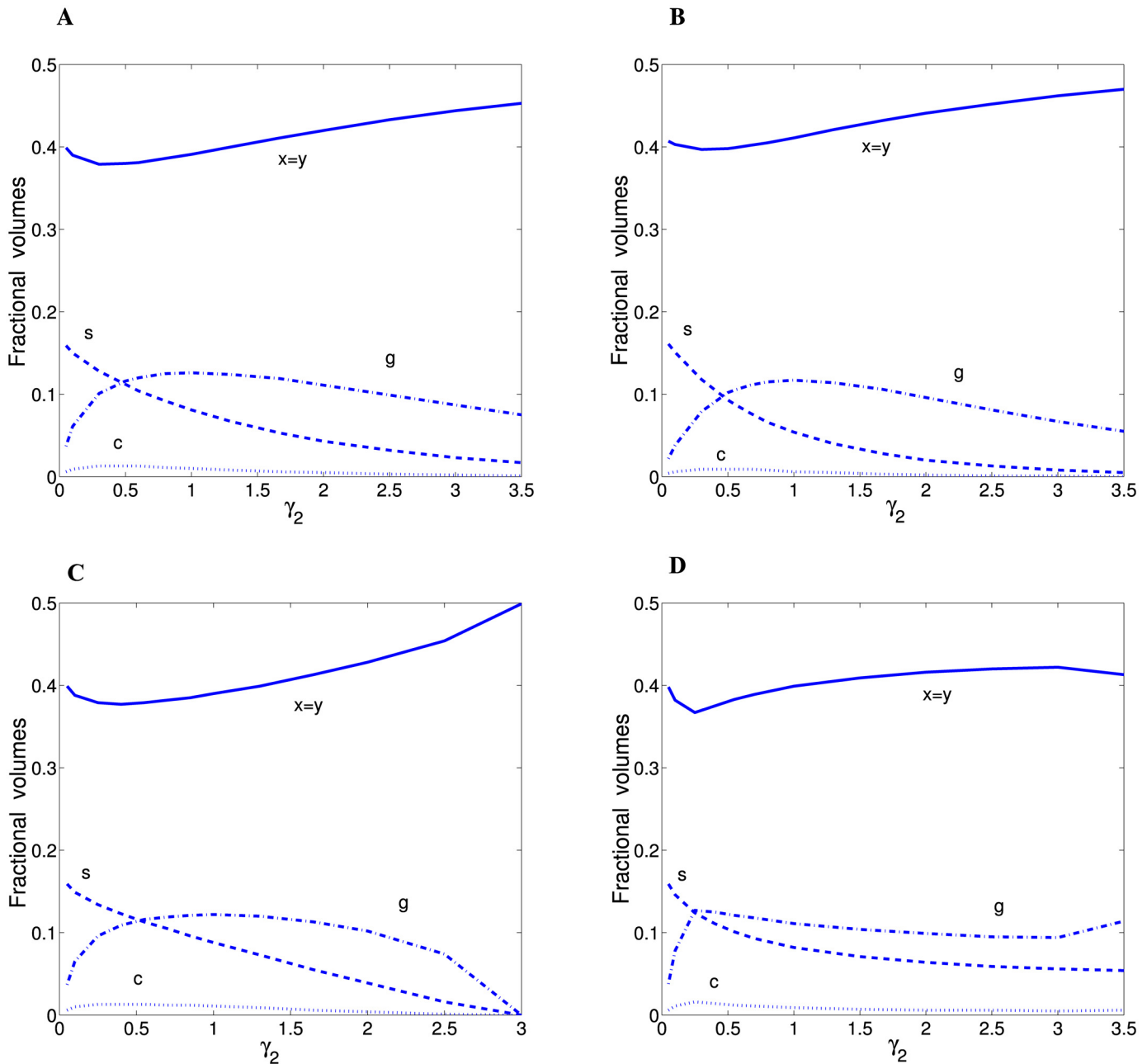
Fig 4. Optimal fractional volumes for "spine economical maximization" principle as functions of the exponent γ_2. The results are qualitatively very similar for (A) Exponential distribution, (B) Gamma ($n = 2$) distribution, (C) Log-logistic distribution ($\beta = 3.0$), and (D) Log-normal distribution ($\sigma = 0.25$). For all distributions $\theta = 0.321 \ \mu m^3$.

doi:10.1371/journal.pcbi.1004532.g004

The degree of similarity between the theory and the data is quantified by two different measures, their Euclidean distance ED, and their Mahalanobis distance MD (see Eqs 34 and 35). The latter is more general, as it takes variability in the data into account. Both measures yield qualitatively very similar results (compare Figs 5 and 6). For wire minimization principle, ED and MD depend biphasically (non-monotonically) on r if $\gamma_1 = 0$ in a similar fashion for all distributions of spine volumes, with characteristic sharp minima for $r \sim 0.95$, for which there are the best matches to the data (Figs 5A and 6A). The overall best results are achieved for Log-
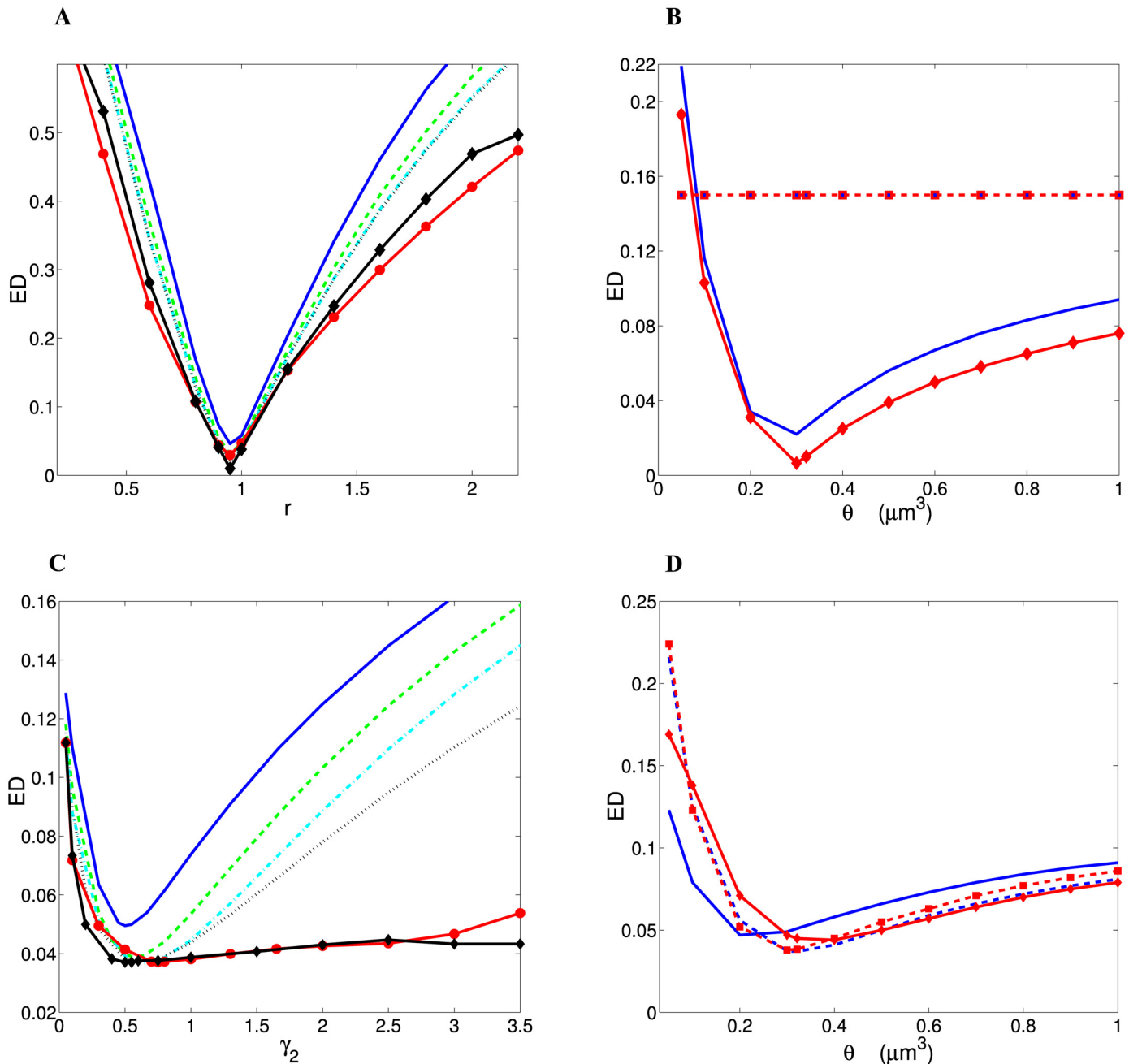
Fig 5. Euclidean distance (ED) between optimal theoretical results and empirical data as a function of r, threshold θ, and γ_1, γ_2. Panels (A) and (B) refer to "wire minimization", whereas panels (C) and (D) correspond to "spine economical maximization". (A) Dependence of ED on r for all distributions of spine volumes for "wire volume minimization", i.e. $\gamma_1 = 0$. (B) ED as a function θ for $r = 0.95$. Blue lines correspond to Gamma ($n = 2$) distribution and red lines (with diamonds and squares) to Log-normal ($\gamma_1 = 0$ for solid lines and $\gamma_1 = 0.65$ for dashed lines). For Log-normal distribution $\sigma = 0.3$. Note that for $\gamma_1 > 0$ ED is constant (dashed red line with blue squares), i.e. ED = 0.15. (C) Dependence of ED on γ_2 for all distributions of spine volumes. (D) ED as a function θ. Blue lines correspond to Gamma ($n = 2$) distribution and red lines (with diamonds and squares) to Log-normal ($\gamma_2 = 0.3$ for solid lines and $\gamma_2 = 0.65$ for dashed lines). For Log-normal distribution $\sigma = 0.25$. In panels (A) and (C) $\theta = 0.321$ μm^3, and the following labels were used: Exponential distribution is shown as solid blue line, Gamma ($n = 1$) and Gamma ($n = 2$) are shown respectively as dashed green and dashdot cyan lines, Rayleigh distribution is represented by dotted black line, Log-logistic is shown as solid red line with circles, and Log-normal as solid black line with diamonds. The curves for Log-logistic and Log-normal correspond to different values of the parameters, respectively, β and σ that yield the minimal ED for a given r or γ_2.

doi:10.1371/journal.pcbi.1004532.g005
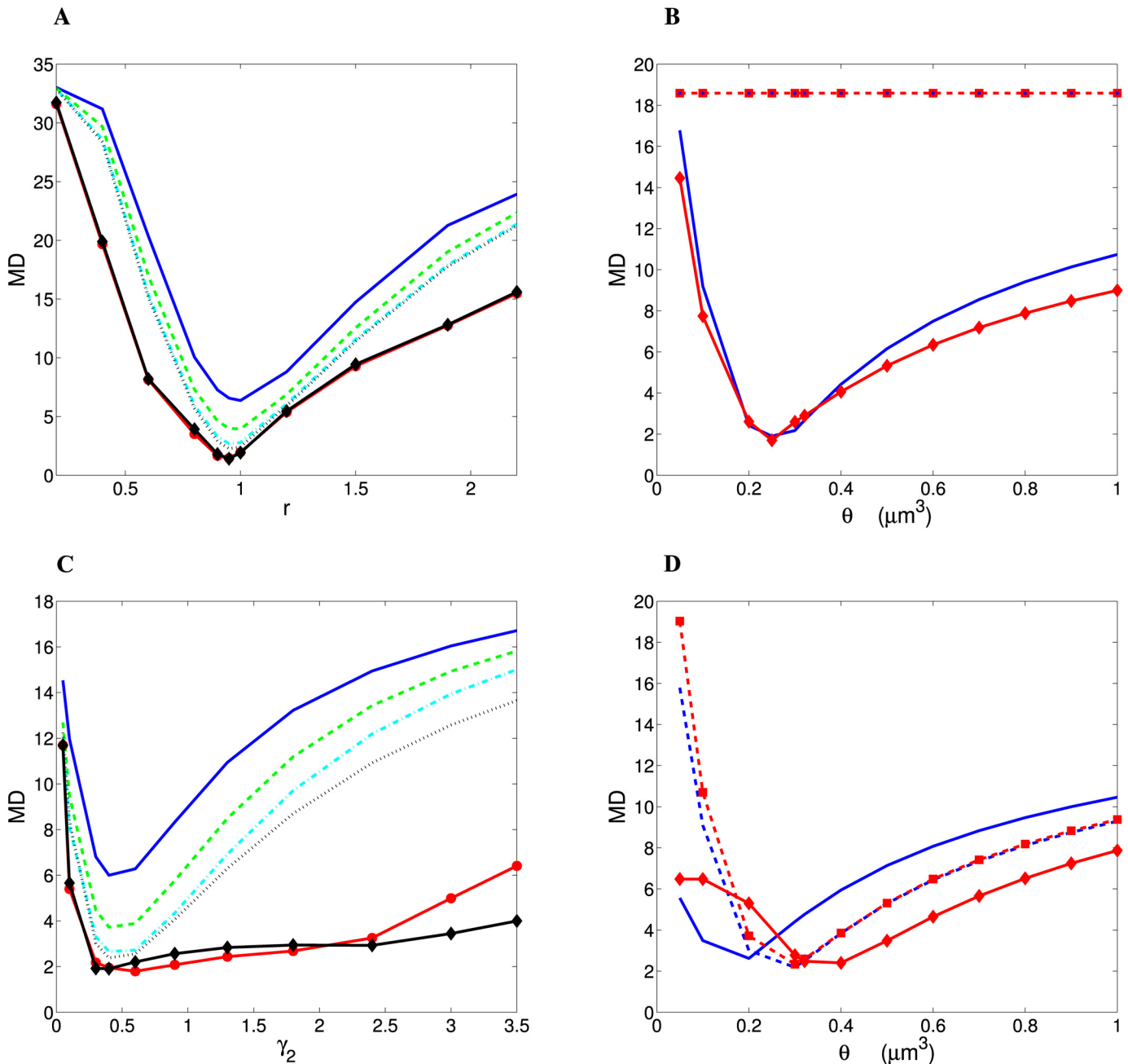
Fig 6. The same as in Fig 5 but for the more general Mahalanobis distance (MD) between optimal theoretical fractions and empirical fractions. (A) MD as a function of r, and (B) MD as a function of θ for wire minimization. (C) MD as a function of γ_2, and (D) MD as a function of θ for spine economical maximization. In panel (D) $\gamma_2 = 0.2$ for solid lines and $\gamma_2 = 0.5$ for dashed lines.

normal distribution (ED = 0.010, MD = 1.405), and other distributions especially those with short-tails produce higher ED and MD (Table 2). Outside the optimal value of r the values of ED and MD grow rather fast, and the agreement between theory and the experiment becomes weak (Figs 5A and 6A). If however, $\gamma_1 > 0$, then ED and MD are both constant and relatively large (ED = 0.15, MD = 18.5), regardless of other parameters and distribution types (Figs 5B and 6B), which implies that similarity with the data is always very weak in this case.

Table 3. The best optimal theoretical fractional volumes and related parameters in the cortex for "spine economical maximization" principle. The optimal fractions correspond to either the minimal Euclidean distance (ED) or Mahalanobis distance (MD) between theory and data (given in bold face).

Spine size distribution	θ	Optimal parameters								ED	MD
		x	y	s	g	c	$\bar{u}$	P	γ_2		
Exponential	0.100	0.374	0.374	0.119	0.118	0.014	0.615	0.850	0.25	**0.043**	1.982
	0.100	0.374	0.374	0.119	0.118	0.014	0.615	0.850	0.25	0.043	**1.982**
	0.321	0.398	0.398	0.093	0.102	0.009	0.599	0.585	0.50	**0.050**	5.913
	0.321	0.397	0.397	0.098	0.097	0.010	0.678	0.623	0.45	0.051	**5.883**
Gamma (n = 1)	0.100	0.366	0.366	0.129	0.123	0.016	0.626	0.959	0.20	**0.051**	2.353
	0.100	0.366	0.366	0.129	0.123	0.016	0.626	0.959	0.20	0.051	**2.353**
	0.321	0.388	0.388	0.098	0.116	0.011	0.520	0.650	0.60	**0.039**	3.886
	0.321	0.385	0.385	0.111	0.107	0.012	0.660	0.746	0.45	0.042	**3.597**
Gamma (n = 2)	0.100	0.370	0.370	0.136	0.110	0.015	0.778	0.993	0.15	**0.056**	2.554
	0.100	0.370	0.370	0.136	0.110	0.015	0.778	0.993	0.15	0.056	**2.554**
	0.321	0.382	0.382	0.101	0.122	0.012	0.495	0.692	0.65	**0.038**	2.914
	0.321	0.380	0.380	0.112	0.116	0.013	0.589	0.774	0.50	0.040	**2.507**
Rayleigh	0.100	0.361	0.361	0.127	0.135	0.017	0.534	0.973	0.20	**0.056**	3.306
	0.100	0.371	0.371	0.136	0.108	0.015	0.806	0.988	0.15	0.056	**2.645**
	0.321	0.380	0.380	0.102	0.125	0.013	0.486	0.710	0.60	**0.038**	2.555
	0.321	0.378	0.378	0.113	0.118	0.013	0.585	0.789	0.45	0.040	**2.284**
Log-logistic	0.100	0.377	0.377	0.106	0.126	0.013	0.498	0.747	0.40	**0.039**	2.152
	0.100	0.377	0.377	0.106	0.126	0.013	0.498	0.747	0.40	0.039	**2.152**
	0.321	0.383	0.383	0.102	0.120	0.012	0.511	0.695	0.75	**0.038**	2.999
	0.321	0.372	0.372	0.114	0.127	0.015	0.524	0.824	0.60	0.043	**1.793**
Log-normal	0.100	0.381	0.381	0.098	0.128	0.013	0.445	0.675	0.30	**0.038**	2.794
	0.100	0.372	0.372	0.120	0.120	0.015	0.603	0.868	0.20	0.045	**1.880**
	0.321	0.383	0.383	0.101	0.121	0.012	0.499	0.688	0.55	**0.038**	3.005
	0.321	0.372	0.372	0.115	0.126	0.014	0.535	0.828	0.35	0.043	**1.788**

For log-logistic distribution the minimal ED and MD were obtained for the parameter $\beta = 1.5$ if $\theta = 0.100$, and if $\theta = 0.321$ then $\beta = 3.0$ for minimal ED and $\beta = 4.0$ for minimal MD. For log-normal distribution the minimal ED and MD were reached for $\sigma = 0.75$ if $\theta = 0.100$, and if $\theta = 0.321$ then $\sigma = 0.25$ for minimal ED and MD.

doi:10.1371/journal.pcbi.1004532.t003

On the other hand, for spine economical maximization ED and MD exhibit minima for γ_2 < 1 (Figs 5C and 6C). Interestingly, neither the minimal values of ED and MD, nor associated with them the optimal values of γ_2 vary much as we change the spine distribution type for a given threshold θ (Figs 5C and 6C). Specifically, the optimal γ_2 is in the range 0.15–0.40 for $\theta =$ 0.100 μm^3, and 0.35–0.75 for $\theta = 0.321$ μm^3 (Table 3). The minima of ED and MD for heavy-tailed distributions are much broader than for short-tailed, which suggests that heavy-tailed distributions can be more flexible in comparison to the data (Figs 5C and 6C). This follows from the fact that heavy-tailed distributions depend on an additional parameter that can be adjusted (Fig. A in Supporting S1 Text). Moreover, the best optimal cortical fractional volumes in Table 3 look very similar across different distributions of spine sizes. ED values for these best solutions are also very similar (Table 3). The smallest possible minimal value of ED is 0.038, and it is reached by four different distributions, independent of the asymptotic tail (Gamma n = 2, Rayleigh, Log-logistic, and Log-normal). (As a comparison, for a hypothetical situation when all theoretical optimal cortical components were uniformly distributed, i.e. each of them were 0.2, we would obtain ED = 0.342, which is about 10 times larger than the actual

minimal ED in Table 3). The situation is different for the MD distance. Despite a high degree of similarity among the optimal fractional volumes across different distributions, MD discriminates these cases much better than ED (Table 3). Distributions having identical ED have in general different MD values (Table 3). The overall trend is such that the best fits to the empirical fractional volumes are given by the distributions of spine sizes with long-tails. The smallest possible minimal MD is achieved for Log-normal distribution (MD = 1.788; Table 3). Because of its higher generality, only the MD measure is used subsequently for comparing theoretical predictions with the data.

The degree of the sensitivity of the optimal cortical fractions on the threshold θ for spine formation is qualitatively mostly similar for both principles of cortical organization considered here (Fig 5B and 5D and Fig 6B and 6D), except for the case of wire minimization with $\gamma_1 > 0$, for which ED, MD, and cortical fractions are independent of θ but are not realistic (Figs 5B and 6B). Indeed, for wire volume minimization (with $\gamma_1 = 0$) and spine economical maximization, ED and MD depend very strongly on θ if $\theta < 0.2\ \mu m^3$ (Figs 5B and 5D and 6B and 6D). However, if $\theta > 0.2\ \mu m^3$ this dependence is milder in both cases (Figs 5B and 5D and 6B and 6D).

Optimal spine sizes and probability of spine formation: Wire minimization vs. spine economical maximization

Optimization of the fitness function F also yields optimal average spine volume $\bar{u}$ and indirectly the conditional probability of spine formation P (see the Methods). We consider the results for pure wire minimization and pure spine economy maximization.

As was previously noted, for wire minimization principle ($f = 1$ in Eq 1) with $\gamma_1 > 0$, we obtain $\bar{u} \mapsto \infty$, and consequently $P = 1$, both of which are unrealistic. For wire minimization with $\gamma_1 = 0$ (wire volume minimization), both $\bar{u}$ and P depend non-monotonically on the parameter r (Fig 7A and 7B). For short-range distributions of spine size, $\bar{u}$ and P are positively correlated, whereas for the distributions with heavy-tails these two quantities are anti-correlated. Thus for wire minimization there is no clear one-to-one correspondence between average spine size and conditional probability of spine formation. Among all the distributions, for the optimal value of r ($r \approx 0.95$), the heavy-tailed Log-normal produces the most realistic spine volume $\bar{u} = 0.24 - 0.56 \mu m^3$, i.e. the closest to the empirical values (0.2–0.4 μm^3 for human and macaque monkey [41, 42]), regardless of the value of threshold θ (Table 2; Fig 7A). For short-tail distributions the values of $\bar{u}$ are strongly threshold θ-dependent (Table 2).

In contrast, for spine economical maximization ($f = 0$ in Eq 1) the quantities $\bar{u}$ and P depend monotonically on the exponent γ_2, and thus are positively correlated for all distributions, i.e. small spine volumes are generally associated with low probabilities P and vice versa (Fig 7C and 7D). For optimal values of γ_2 (< 1) the average spine volumes have very similar values regardless of the spine size distribution and the threshold θ (Gamma n = 2 and Rayleigh distributions are exceptions), typically: $\bar{u} = 0.44 - 0.67 \mu m^3$ (Table 3), which is also close to the experimental data [41, 42].

Optimal fractional volumes of cortical components: Combined "wire min and spine max" meta-principle

Now we consider the scenario when wire minimization and spine economical maximization notions are mixed together simultaneously, and optimal fractional volumes are obtained by minimization of the meta fitness function in Eq (1) with the control parameter $0 < f < 1$. In general, the best results in terms of agreement with the empirical data are reached for the cases when spine economy rule dominates in the meta fitness function, i.e. $f \ll 1$, (Fig 8; Tables 4–6). More precisely, MD distance has very shallow minima in the range $f \sim 0.1$–0.3 (Fig 8). The
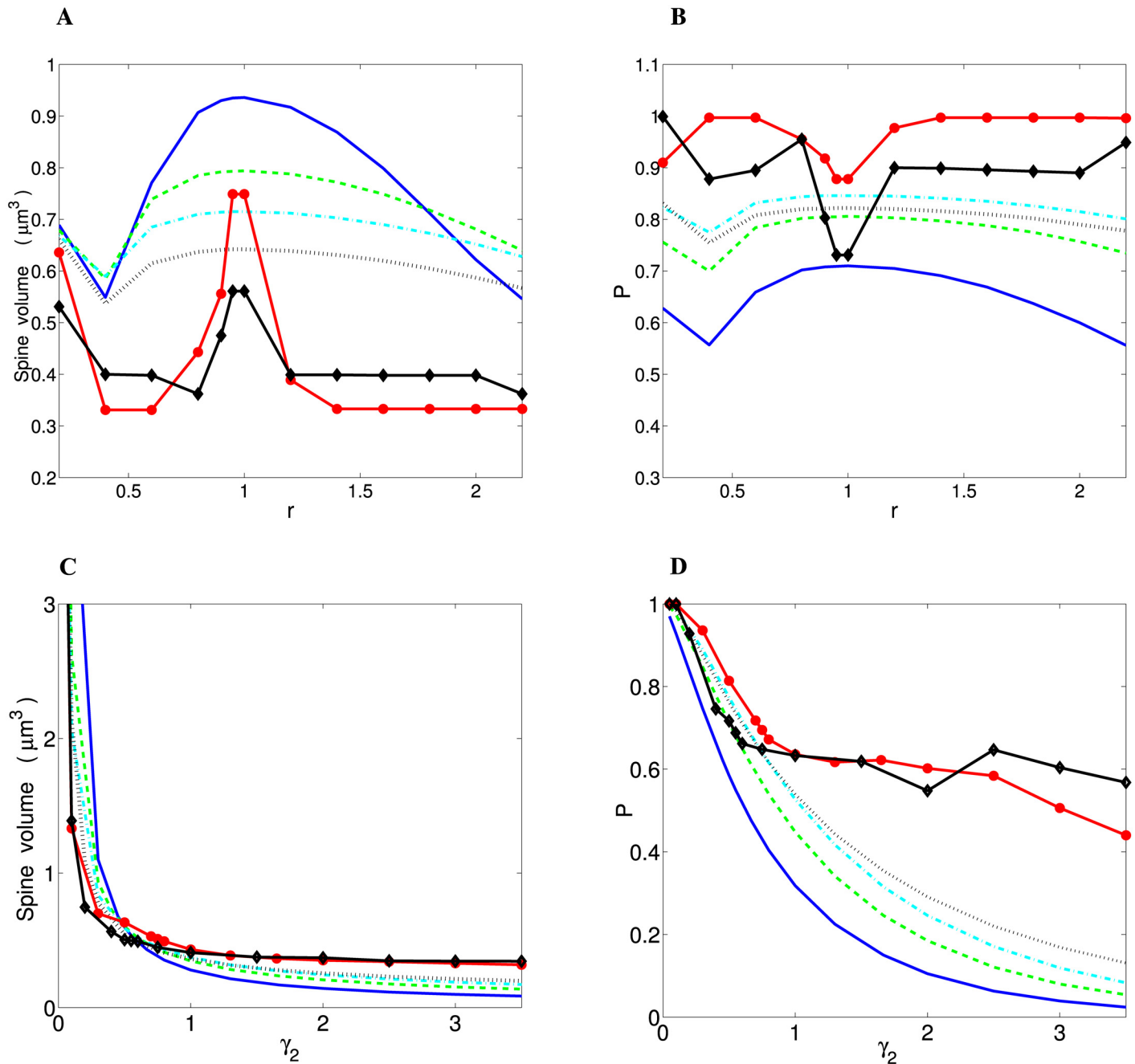
Fig 7. Optimal average spine volume $\overline{u}$ and conditional probability of spine formation P for different distributions of spine sizes. Panels (A) and (B) refer to "wire volume minimization", whereas panels (C) and (D) correspond to "spine economical maximization". (A) Non-monotonic dependence of spine volume $\overline{u}$ and (B) conditional probability P on r for wire fractional volume minimization ($\gamma_1 = 0$). (C) Spine volume $\overline{u}$ and (D) conditional probability P decrease monotonically with increasing the exponent γ_2. For all panels the same labels for curves corresponding to a given distribution were used, and they are identical to the labels used in Fig 5A and 5C. The curves for Log-logistic and Log-normal correspond to different values of the parameters, respectively, β and σ that yield the minimal ED for a given r or γ_2. For all panels $\theta = 0.321 \ \mu m^3$.

doi:10.1371/journal.pcbi.1004532.g007
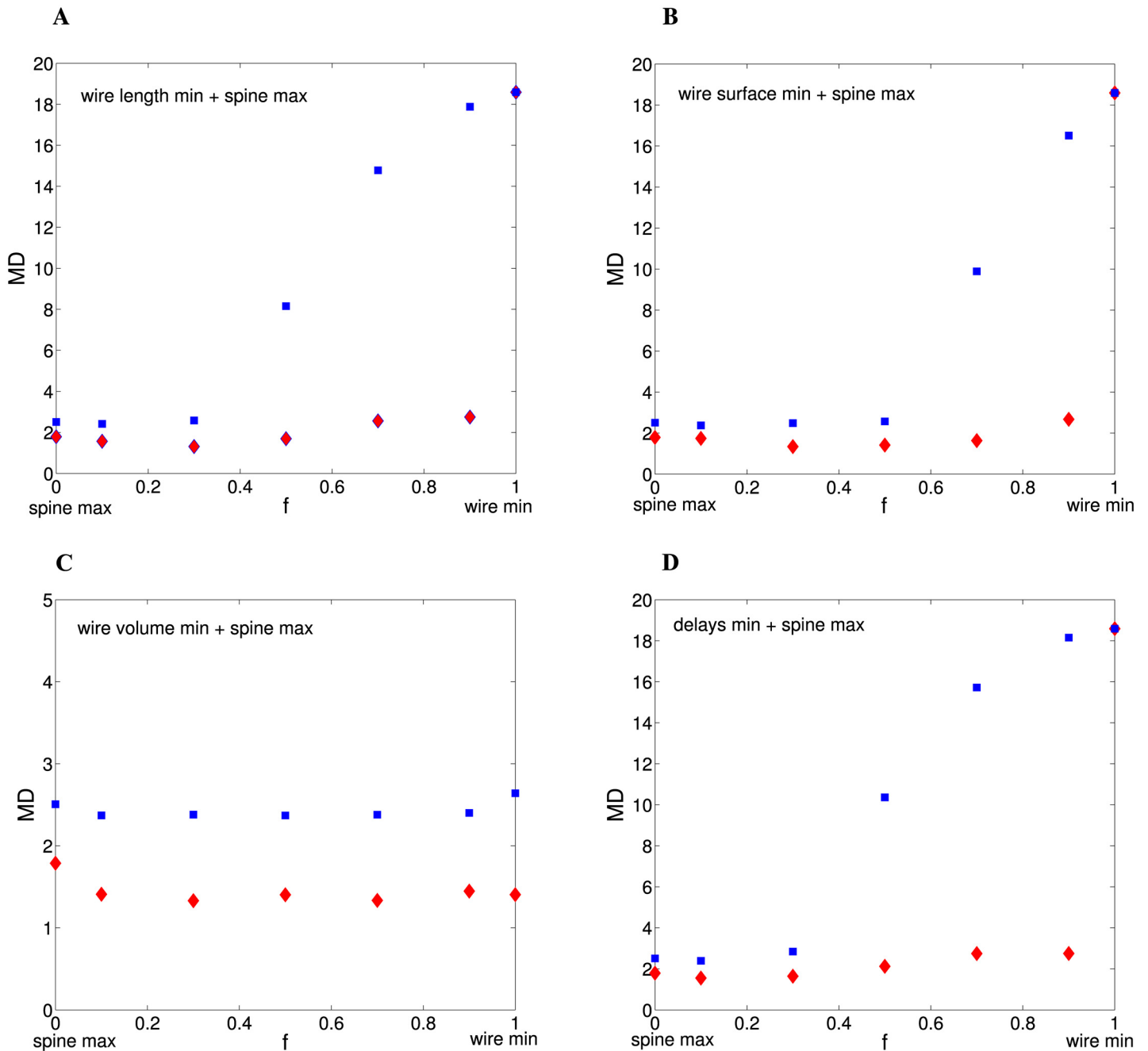
Fig 8. The minimal value of MD as a function the control parameter _f_ for the combined "spine economy max and wire min" principle. Blue squares correspond to Gamma (n = 2) distribution of spine sizes and red diamonds to Log-normal distribution. The notion of spine economy max is mixed with different types of wire cost min principle: wire length in (A), wire surface area in (B), wire volume in (C), and conduction delays in (D). In almost all panels MD has extremely shallow minima for $f \sim 0.1$–0.3, and then MD increases either weakly or abruptly as _f_ increases further (for $f = 1$ MD is the same for both distributions of spine sizes). The exception is the mixture of wire volume min and spine max (panel C), where MD is practically constant. For all panels $\theta = 0.321 \ \mu m^3$.

doi:10.1371/journal.pcbi.1004532.g008

Table 4. The best optimal theoretical fractional volumes and related parameters in the cortex for the combined "wire min + spine max" principle with control parameter f = 0.1. The optimal fractions correspond to the minimal Mahalanobis distance (MD) between theory and data.

Principle type/spine distr.	Optimal parameters									MD
	x	y	s	g	c	$\bar{u}$	P	r	γ_2	
Wire length min + spine max (γ_1 = 2/3)										
Exponential	0.399	0.396	0.097	0.098	0.010	0.655	0.612	0.99	1.00	5.885
Gamma (n = 1)	0.395	0.377	0.107	0.110	0.012	0.612	0.717	0.90	0.95	3.558
Gamma (n = 2)	0.393	0.368	0.110	0.117	0.013	0.569	0.759	0.85	0.95	2.416
Rayleigh	0.395	0.362	0.110	0.120	0.013	0.553	0.768	0.80	0.90	2.117
Log-logistic	0.400	0.344	0.116	0.126	0.015	0.544	0.844	0.65	0.90	1.277
Log-normal	0.386	0.353	0.112	0.134	0.015	0.480	0.825	0.80	0.80	1.565
Wire surface min + spine max (γ_1 = 1/3)										
Exponential	0.402	0.393	0.100	0.096	0.010	0.696	0.631	0.95	0.70	5.903
Gamma (n = 1)	0.394	0.377	0.108	0.109	0.012	0.629	0.728	0.90	0.70	3.549
Gamma (n = 2)	0.396	0.364	0.111	0.116	0.013	0.589	0.774	0.80	0.70	2.375
Rayleigh	0.399	0.358	0.111	0.118	0.013	0.576	0.784	0.75	0.65	2.105
Log-logistic	0.398	0.346	0.117	0.125	0.015	0.550	0.850	0.65	0.70	1.280
Log-normal	0.396	0.347	0.104	0.138	0.014	0.423	0.759	0.65	0.80	1.741
Wire volume min + spine max (γ_1 = 0)										
Exponential	0.399	0.396	0.099	0.096	0.010	0.692	0.629	0.98	0.45	5.898
Gamma (n = 1)	0.398	0.374	0.107	0.110	0.012	0.617	0.721	0.85	0.50	3.553
Gamma (n = 2)	0.395	0.365	0.112	0.115	0.013	0.598	0.781	0.80	0.50	2.371
Rayleigh	0.397	0.359	0.113	0.117	0.013	0.590	0.792	0.75	0.45	2.111
Log-logistic	0.399	0.345	0.117	0.125	0.015	0.548	0.848	0.60	0.55	1.277
Log-normal	0.400	0.343	0.110	0.133	0.015	0.474	0.798	0.60	0.45	1.409
Delays min + spine max (γ_1 = 5/6)										
Exponential	0.398	0.398	0.096	0.099	0.010	0.642	0.606	1.00	1.15	5.887
Gamma (n = 1)	0.390	0.382	0.106	0.111	0.012	0.597	0.708	0.95	1.10	3.588
Gamma (n = 2)	0.393	0.367	0.111	0.117	0.013	0.580	0.768	0.85	1.05	2.393
Rayleigh	0.392	0.366	0.108	0.121	0.013	0.537	0.755	0.85	1.05	2.164
Log-logistic	0.396	0.348	0.114	0.127	0.014	0.530	0.830	0.70	1.05	1.295
Log-normal	0.390	0.356	0.108	0.132	0.014	0.469	0.775	0.80	1.00	1.553

All the results correspond to θ = 0.321.

doi:10.1371/journal.pcbi.1004532.t004

worst results are found for the cases when wire minimization rule prevails ($f \mapsto 1$), and intermediate results are obtained for the balanced case when spine economy max and wire min are treated with equal weights, i.e. $f \sim 0.5$ (Fig 8 and Tables 4–6). However, there is an exception to this tendency, namely, the mixture of wire volume minimization and spine economy maximization, which yields invariant results and good similarity with the data regardless of the value of mixing ratio f (Fig 8C and Tables 4–6).

For the case when spine economy predominates (f = 0.1) in F, we obtain that mixing spine max with a small fraction of any type of wire min rule (arbitrary γ_1) gives essentially the same results for MD (Table 4), and they are very similar to the results for pure wire volume minimization (Table 2) and pure spine economy maximization (Table 3). This means that for this particular scenario all kinds of wire minimization rule, such as length min, surface area min, volume min, or delays min, are equally reasonable, but they are less important than spine economy. This, however, is not the case when wire minimization prevails in the mixing of notions,

Table 5. The best optimal theoretical fractional volumes and related parameters in the cortex for the combined "wire min + spine max" principle with control parameter *f* = 0.5. The optimal fractions correspond to the minimal Mahalanobis distance (MD) between theory and data.

Principle type/spine distr.	Optimal parameters									MD
	x	*y*	*s*	*g*	*c*	$\overline{u}$	*P*	*r*	γ_2	
Wire length min + spine max ($\gamma_1 = 2/3$)										
Exponential	0.453	0.453	0.013	0.080	0.001	0.115	0.061	1.00	2.95	15.22
Gamma (n = 1)	0.421	0.433	0.036	0.107	0.004	0.212	0.195	1.05	2.75	11.75
Gamma (n = 2)	0.399	0.413	0.059	0.121	0.007	0.290	0.356	1.05	2.60	8.157
Rayleigh	0.393	0.407	0.065	0.127	0.008	0.299	0.405	1.05	2.55	7.047
Log-logistic	0.392	0.359	0.099	0.137	0.014	0.409	0.706	0.90	2.40	2.118
Log-normal	0.399	0.353	0.110	0.125	0.014	0.520	0.777	0.90	2.10	1.692
Wire surface min + spine max ($\gamma_1 = 1/3$)										
Exponential	0.421	0.421	0.040	0.114	0.005	0.215	0.225	1.00	2.00	10.94
Gamma (n = 1)	0.395	0.395	0.079	0.122	0.010	0.389	0.509	1.00	1.85	5.508
Gamma (n = 2)	0.380	0.380	0.109	0.118	0.013	0.558	0.751	1.00	1.70	2.566
Rayleigh	0.392	0.368	0.102	0.125	0.013	0.486	0.710	0.95	1.65	2.436
Log-logistic	0.404	0.336	0.114	0.131	0.015	0.500	0.835	0.85	1.60	1.350
Log-normal	0.395	0.347	0.110	0.133	0.015	0.475	0.804	0.90	1.40	1.414
Wire volume min + spine max ($\gamma_1 = 0$)										
Exponential	0.398	0.398	0.097	0.098	0.010	0.655	0.613	1.00	0.55	5.886
Gamma (n = 1)	0.403	0.369	0.107	0.109	0.012	0.617	0.721	0.95	0.60	3.566
Gamma (n = 2)	0.395	0.364	0.112	0.115	0.013	0.598	0.781	0.95	0.60	2.370
Rayleigh	0.394	0.363	0.111	0.119	0.013	0.567	0.777	0.95	0.55	2.107
Log-logistic	0.400	0.344	0.116	0.126	0.015	0.544	0.844	0.90	0.70	1.278
Log-normal	0.401	0.340	0.111	0.133	0.015	0.478	0.816	0.90	0.40	1.403
Delays min + spine max ($\gamma_1 = 5/6$)										
Exponential	0.463	0.463	0.008	0.065	0.001	0.097	0.036	1.00	3.40	16.15
Gamma (n = 1)	0.438	0.438	0.026	0.096	0.002	0.183	0.135	1.00	3.10	13.34
Gamma (n = 2)	0.419	0.419	0.045	0.113	0.005	0.249	0.257	1.00	2.95	10.36
Rayleigh	0.410	0.410	0.053	0.121	0.006	0.265	0.317	1.00	2.90	8.918
Log-logistic	0.396	0.345	0.105	0.139	0.015	0.420	0.765	0.85	2.50	1.761
Log-normal	0.405	0.337	0.100	0.144	0.014	0.383	0.732	0.80	2.40	2.124

All the results correspond to $\theta = 0.321$.

doi:10.1371/journal.pcbi.1004532.t005

or when there is a balance between them (cases *f* = 0.9 and *f* = 0.5, respectively). In these scenarios, wire volume min (and occasionally wire surface min) gives noticeably better results than either wire length min or delays min (Tables 5 and 6). However, it has to be stressed that mixing together spine economy rule with any of the wire cost rules with $\gamma_1 > 0$ (wire length, wire surface, delays), at any ratio, always gives better results than for these wire cost rules alone, i.e., for *f* = 1 (Fig 8A, 8B and 8D).

Another interesting feature of the results in Tables 4–6 is that the best agreements with the data are almost always recorded for the distributions of spine sizes with long tails. This trend is conserved for a large spectrum of the values of *f*, however, as $f \mapsto 1$ (the notion of wire min dominates in *F*) the similarity to the data becomes weaker or even non-existent (see Fig 8 for Log-normal distribution).

To summarize, mixing the rules of spine economy max with wire min does not give significantly better results than for pure spine economy max or pure wire volume min. At best, such a

Table 6. The best optimal theoretical fractional volumes and related parameters in the cortex for the combined "wire min + spine max" principle with control parameter $f = 0.9$. The optimal fractions correspond to the minimal Mahalanobis distance (MD) between theory and data.

Principle type/spine distr.	Optimal parameters									MD
	x	y	s	g	c	$\overline{u}$	P	r	γ_2	
Wire length min + spine max ($\gamma_1 = 2/3$)										
Exponential	0.414	0.414	0.172	0.000	0.000	22077.8	1.000	1.00	0.10	18.45
Gamma (n = 1)	0.489	0.489	0.001	0.020	0.000	0.086	0.005	1.00	6.40	18.33
Gamma (n = 2)	0.484	0.484	0.003	0.029	0.000	0.118	0.012	1.00	6.20	17.88
Rayleigh	0.471	0.471	0.008	0.050	0.000	0.157	0.038	1.00	6.10	16.69
Log-logistic	0.414	0.414	0.172	0.000	0.000	22073.2	1.000	1.00	0.10	18.45
Log-normal	0.401	0.340	0.093	0.151	0.014	0.332	0.684	0.35	5.50	2.751
Wire surface min + spine max ($\gamma_1 = 1/3$)										
Exponential	0.487	0.487	0.001	0.025	0.000	0.060	0.005	1.00	5.20	18.13
Gamma (n = 1)	0.478	0.478	0.004	0.040	0.000	0.107	0.018	1.00	4.90	17.38
Gamma (n = 2)	0.468	0.468	0.009	0.054	0.001	0.146	0.040	1.00	4.65	16.51
Rayleigh	0.454	0.454	0.017	0.074	0.001	0.181	0.084	1.00	4.60	15.07
Log-logistic	0.402	0.339	0.095	0.150	0.014	0.341	0.696	0.75	4.20	2.622
Log-normal	0.402	0.347	0.092	0.145	0.013	0.348	0.664	0.85	3.80	2.670
Wire volume min + spine max ($\gamma_1 = 0$)										
Exponential	0.398	0.398	0.097	0.099	0.010	0.651	0.611	1.00	1.10	5.886
Gamma (n = 1)	0.386	0.386	0.108	0.109	0.012	0.628	0.728	1.00	1.20	3.591
Gamma (n = 2)	0.404	0.355	0.112	0.115	0.013	0.601	0.783	0.95	1.20	2.401
Rayleigh	0.403	0.354	0.111	0.119	0.013	0.568	0.779	0.95	1.00	2.126
Log-logistic	0.394	0.350	0.114	0.127	0.015	0.529	0.829	0.95	1.60	1.311
Log-normal	0.396	0.349	0.109	0.132	0.014	0.472	0.788	0.95	0.70	1.447
Delays min + spine max ($\gamma_1 = 5/6$)										
Exponential	0.425	0.403	0.171	0.001	0.000	2095.2	1.000	0.50	0.10	18.37
Gamma (n = 1)	0.425	0.403	0.171	0.001	0.000	2091.7	1.000	0.50	0.10	18.37
Gamma (n = 2)	0.487	0.487	0.002	0.024	0.000	0.111	0.008	1.00	6.70	18.15
Rayleigh	0.475	0.475	0.006	0.043	0.000	0.151	0.029	1.00	6.70	17.11
Log-logistic	0.425	0.403	0.171	0.001	0.000	2091.7	1.000	0.50	0.10	18.37
Log-normal	0.401	0.340	0.093	0.151	0.014	0.332	0.684	0.40	5.60	2.751

All the results correspond to $\theta = 0.321$.

mixing yields marginally better results, but only if the spine component prevails ($f \ll 1$) in the meta fitness function F.

Discussion

Hierarchy in cortical composition and the rule "powers of 1/3"

Experimental data analyzed in this paper indicate that the distribution of the basic components in the gray matter of cerebral cortex is relatively stable across mammalian species (Table 1; Fig 2). Axons and dendrites occupy on average similar fractions $\sim 1/3$ of cortex volume, spines and glia/astrocytes take each about 1/10 of the cortex, and capillaries constitute roughly $\sim 1/100$ of the cortical space. These numbers in themselves are interesting, because they form a special hierarchy of dependencies, being approximately integer powers of 1/3 (Fig 1). Specifically, the content of spines or glia/astrocytes is roughly equal to the square of axon (or dendrite) content, and capillary content in turn is approximately equal to the square of spine content

([Table 1]). This component hierarchy may be somehow important for efficient cortical computation, and thus worth investigating.

Summary of the main theoretical results: The importance of spine economy principle

Hierarchy in cortical composition was a motivation for theoretical considerations about principles governing organization of the cerebral cortex. The goal was to provide a theoretical explanation of this hierarchy starting from a neurobiologically plausible yet simple principle. Two basic principles are considered: different forms of a standard neural wire minimization [3, 7–9, 43], and the new one proposed here called spine economical maximization. The latter rule is related to maximization of spine content in the cortex with simultaneous minimization of average spine size (which is supposed to reduce the metabolic cost). We also study a mixture of the two principles as a meta principle. The optimal outcomes of these models are compared to the experimental data, using two similarity measures (Euclidean and Mahalanobis distances).

This study shows that from many implementations of wire minimization concept, only the minimization of wire fractional volume ($\gamma_1 = 0$) can give reasonable results that are close to the experimental data, if a free parameter (r in [Eq 21]) is chosen appropriately (compare Tables [1] and [2]; Figs [5A] and [6A]). The other possibilities related to wire minimization (with $\gamma_1 > 0$), such as minimization of wire length, its area, or conduction delays, yield unrealistic results: zeros for volume fractions of glia/astrocytes and capillaries ([Fig 3A and 3C]), resulting in relatively high values of ED and MD (Figs [5B] and [6B]), and infinite values of the average spine volume, which is clearly wrong. The last result follows from the fact that the minimal value of F_w in [Eq (21)] is precisely zero, which takes place only for $\bar{u} = \infty$ (other possibility with vanishing of axonal x and dendritic y fractions is forbidden, since that would imply that all fractions are zero, which would violate the fractions normalization constraint represented by [Eq (31)]).

On the other hand, the principle of spine economic maximization produces the fractional cortical volumes that are also close to the data (compare Tables [1] and [3]), but they do not require such a careful tuning of a free parameter (γ_2 in [Eq 24]), especially for the distributions of spine volume with heavy-tails (compare the scales in [Fig 5C vs. 5A] and in [Fig 6C vs. 6A]). Thus, both principles provide quantitatively similar results, however, maximization of the simple benefit-cost function F_s with spine content in the centerpiece (see [Eq 24]) produces a more robust outcome. This conclusion is consistent with suggestions that neural systems are not exclusively optimized for minimal wiring length or component placement [15, 16], and other factors or their combinations can be also involved [11–16]. This suggests that economic spine content maximization can possibly provide an additional and/or alternative mechanism that is used by evolution to regulate the efficiency of cortical circuits.

As a third possibility we consider the meta principle that combines spine economy with wiring cost, with some mixing ratio f. This mixing scenario improves greatly the results associated with minimization of wire length, wire surface area, and temporal delays ($\gamma_1 > 0$), by making MD distances much smaller, but only when the spine economy dominates in the mixing of notions in the fitness function ([Eq 1]). Thus, clearly the presence of the principle of spine economical maximization is necessary to make the concepts of wire length and temporal delays minimizations to be relevant candidates for the explanation of cortical composition hierarchy ([Table 4]). However, it must be emphasized that mixing of wire volume min ($\gamma_1 = 0$) with spine economy max does not produce noticeably better results (only a tiny improvement) in comparison to the cases when these two principles act in isolation ([Fig 8C]).

Finally, for all three scenarios (either $f = 0$, $f = 1$, or f between 0 and 1 in [Eq 1]), the best theoretical fractional volumes are generally obtained for distributions of spine volume with heavy-

tails (Tables [2]–[6]). In addition, many of these best solutions give optimal average spine volumes $\bar{u}$, which despite some variability, are in good agreement with experimental values, which are 0.35 μm^3 for human [41], and 0.3–0.4 μm^3 for macaque monkey [42]. Spine size correlates with synaptic weight [19], and hence variability in spine size that is observed among the best solutions is a positive feature, because it implies variability in synaptic weights, which in turn is necessary for brain function.

The models for pure wire volume minimization and for pure spine economy differ strongly in their predictions regarding the relationship between average spine size and conditional probability of spine formation P ([Fig 7A and 7B] vs. [Fig 7C and 7D]). While for wire volume minimization there is no clear one-to-one correspondence, for spine economy we obtain that small spines are associated with small P ([Fig 7C and 7D]). This means that for the latter principle very small spines are unlikely to form and thus are highly stochastic, even when an axon and dendrite are very close to each other. In contrast, large spines with sufficiently large energy capacity have high probability of forming stable synapses. Mathematically, this effect is achieved in the model by introducing the threshold θ for spine volume (see [Eq 3] in the [Methods]). This theoretical result for spine economical maximization is in line with experimental observations, indicating high stochastic motility of small spines and structural stability of larger ones [19, 44–47].

Previous directly related work

In the past there was only one directly related work associated with cortical composition and its theoretical basis [8]. In that study, the authors analyze only the combined optimal fractional volume of axons and dendrites (called wire), which turns out to be close to the empirical value. Chklovskii et al [8] used specific "thought experiments" to demonstrate that the optimal wire fraction can be derived from several equivalent principles, such as minimization of conduction delays, minimization of wiring length, and maximization of synaptic density. The present study is similar in spirit, i.e. in the expectation that fractional volumes are the result of some evolutionary optimization, but differs in the scope and details of what is actually optimized. Apart from considering different forms of wire minimization, we also investigate a new principle of spine economy, and its combination with wire cost (meta principle represented by [Eq 1]), and all three are analyzed in much more detail than in [8]. In particular, in this work we study five cortical components both neuronal and non-neuronal, in contrast to [8], who considered only a simple division wire vs. non-wire. Moreover, we provide explicit formulae for fractional volumes of different components and their mutual couplings, based on a concept of geometric probability, efficient transport for astrocytes, and some neuroanatomical observations.

Other formulations of the problem related to spine economy

One may wonder why in the fitness function related to spine economy ([Eq 24]), the spine proportion (s) is maximized instead of (maybe more natural) numerical spine density (ρ_s)? In fact, both possibilities are included in the fitness function, since these two quantities are linearly related ($s = \rho_s \bar{u}$). Thus the fitness function ([Eq 24]) can be equivalently written as $F_s \sim \rho_s / \bar{u}^{\gamma_2 - 1}$, with the renormalized power of $\bar{u}$. However, since the best results are obtained for $\gamma_2 < 1$, this new formulation implies that spine density and average spine volume both would have to be maximized, i.e., there would be no penalty on spine size. Thus, the original fitness function with spine proportion s seems to better capture the energy constraint, which suggests that s is a more primary variable than ρ_s.

Organization of local vs global circuits

This study considers local cortical circuits, presumably corresponding to a cortical column in size, and does not address the large-scale organization of the mammalian brain. In a present mathematical formulation of local circuits the notion of spatial scale is not taken explicitly into account. This is justified by the fact that locality means that all elements are sufficiently close to each other so that there should not be large detrimental delays in their communication. That temporal delays are not critical in local networks follows from a fact that diameters of intracortical axons and dendrites, directly related to velocities of propagated signals along them [48], are invariant with respect to brain size [14]. The situation is different for global long-range connections via white matter, which show a slight increase in average axon diameter with brain size [49]. Moreover these axons are myelinated, which enhances several-fold the speed of signal propagation in comparison to unmyelinated intracortical axons. These empirical facts indicate that for global brain organization the distance and delays are important constraints, and they were repeatedly used by many researchers to model large-scale organization of brain connectivity [7, 10, 15–17, 50]. Some of these studies initially showed that certain parts of the nervous system in macaque monkey (prefrontal areas) and in the nematode *C. elegans* are optimized for wiring length [7, 10, 50]. However, more recent studies demonstrated that wire length was not fully minimized across macaque and cat visual areas [17], and more importantly, global connections in the whole networks of macaque and *C. elegans* brains are far from being optimal for wire cost [15, 16]. The latter studies indicate that there might be other constraints on global brain organization, such as the requirement of short processing paths, which was proposed in the past [51], or some other combinations [3, 11–14].

The important issue is how to relate local organization in the cortex to global cortico-cortical connectivity. This is a challenging task, not only conceptually, but also from a methodological point of view. The approach presented here for the description of local networks relies on analytical optimization of Lagrange functions, and it differs considerably from the approaches used for studying patterns of long-range connections, which use mainly numerical algorithms of graph theory [13, 15, 16]. It is not clear how to combine the two approaches within a single mathematical framework. However, despite these technical difficulties, there is at least one quantity that can relate local and global organizations. This quantity is associated with the fraction of axons in the cortex x, which is composed of two contributions: local intracortical axons and endings of the long-range axons (via white matter). Empirical data indicate that the latter component is substantial [52], and it seems to be possible to find a mathematical formula relating the two contributions. Since the long-range part of x should be somehow correlated with the volume of axons in white matter, it may be feasible to make a connection between variables operating locally with those operating globally. In particular, one might try to derive from "first principles" the scaling relation between volumes of gray and white matters.

Generalization of the optimality models

The principle of spine economy maximization (as well as other principles) was defined locally in this paper. This means that spatial correlations between different cortical components were neglected. One natural extension of this work is to include spatial dependence in the fitness functions (Eqs 1, 21 and 24), by considering more local circuits with slightly different properties that are coupled together. Such an approach would allow us, in principle, to model spatial plasticity effects and competition for space in the cortex. For example, it is known that learning modifies the structure of spines [19], and there are some indications that it also alters dendritic and axonal processes [53]. The interesting question here is how these two types of modifications are related to one another, and how they influence neighboring circuits.

Another possible extension is to include explicitly the temporal aspect in the equations. The current approach, without time, describes a mature "average" brain. Time dependence of cortical composition would allow us to model the effects associated with brain development. In particular, there are data on synaptic density development in different parts of the cortex across species (references in [27]). Many of these dependencies show that synaptic density acquires a maximum at some early developmental stage, and then it decays to adult (stable) values. It would be interesting to see if spine economy rule combined with time can generate such non-monotonic dependencies. The temporal aspect in the equations could formally be included in analogy with a Hamiltonian approach known from classical mechanics [54], i.e. the fitness function F_s could serve as a Hamiltonian of the local circuit.

Conclusions

This study shows that hierarchical composition of local cortical circuits can be best explained by two different design principles. One is associated with a new proposition called here spine economical maximization, and another with neural wire volume minimization, and both give similar the best optimal solutions. In contrast, other principles related to wire minimization such as: wire length, wire surface area, or conduction delays minimizations do not yield reasonable results. Only when combined with spine economy rule, these other notions can equally well be fitted to the data under some conditions (spine economy contribution must dominate in the mixing of concepts in the meta-fitness function and/or spine size distribution must have a long tail). These results imply that for the efficiency of local circuits (i) wire volume may be more basic variable than wire length or temporal delays, (ii) spine economy principle may be an important concept, and (iii) we should pay more attention to spines, especially in a broader context of brain evolutionary design.

METHODS

Data gathering and analysis for cortical composition

The ethics statement does not apply to this study. Experimental data in Table 1 for cortical composition come from different sources. They are either directly taken from a source or calculated based on other related neuroanatomical data.

Mouse data. Data from [38], except for capillaries—data from [29].

Rat data. Data from [55], except for capillaries—data from [56].

Rabbit data. Fractional volumes are arithmetic means of the values for cortical spaces between and within dendrite bundles in the visual cortex of layers 2 and 3 [57].

Cat data. Density of axon length and dendrite length near the layer 3/4 of visual cortex was estimated as respectively 3.93 ± 0.8 μm/μm^3 and 0.39 ± 0.08 μm/μm^3 [52]. The fractional volumes of axons and dendrites were obtained by assuming axon and dendrite diameters as respectively 0.3 μm [38] and 1.0 μm [58]. Astrocyte data come from [59], and capillary data from [60].

Macaque monkey data. The fractional volume of dendrites was estimated in prefrontal cortex as 0.33 ± 0.19, based on the formula: $(\pi/4)\rho_n \, l_d d^2$, where the neuron density $\rho_n = (1.0 \pm 0.2)$ 10^5 mm^{-3} [61], average total dendrite length per neuron l_d = 3478 ± 99 μm [62], and average dendrite diameter d = 1.1 ± 0.2 μm [63, 64]. The volume fraction of spines was estimated as a product of average spine head volume 0.15±0.01 μm^3 (probably an underestimate for a whole spine volume) and spine density 0.30 ± 0.03 μm^{-3} in prefrontal cortex [65]. Capillary fraction data come from visual cortex [30].

Human data Average spine volume (cingulate cortex) is 0.35±0.02 μm^3 [41] and density of asymmetric synapses (temporal cortex), presumably spines, is $(4.23 \pm 2.59)10^{-1}$ μm^{-3} [66].

Average fraction of spine volume was estimated as the product of these two parameters. The ratio of cortical volumes taken by dendrites and by spines is 2.39, which comes from dividing total volumes of basal and apical dendrites (424.5 μm^3) and spines (177.3 μm^3) per neuron in cingulate cortex of 40 years old human [41]. The volume fraction of dendrites was estimated as a product of 2.39 and the volume fraction of spines. Astrocyte and capillary fractions data come from parietal cortex [67].

Theoretical modeling

To find the optimal structural layout of the mature cerebral cortex we slightly simplify the analysis and consider its five major components that seem to be functionally important: axons, dendrites, spines, glia/astrocytes, and capillaries. In the considerations below we rely on a concept of geometric probability, which relates fractional volumes of cortical components with average probabilities of their encountering. In this mean-field approach, the details of neuronal or glial arborizations are not important.

Model of spine fractional volume. In a mature brain axons and dendrites are much more structurally stable than synapses (spines), which can change volume or even disappear relatively fast [44–47]. Consequently, it is assumed that axonal and dendritic fractions form two primary independent variables that set to a large degree the cortical layout. A third, independent variable is an average spine volume. Spine size is indirectly related to the amount of metabolic energy it uses, through Na/K-ATPase pumps located on spine membrane [21]. Bigger spines with larger surface area require more energy for pumping out Na$^+$ ions and maintaining their concentration gradient than smaller spines. There is some evidence that dendritic spines are the major energy users in the cortex [25–27], and thus, their energy or alternatively their volume, seems to be an important variable. In this study, we focus explicitly on spine volume as an independent variable instead of spine energy, since there exist data on the distribution of spine sizes [41, 68, 69] or spine EPSP [70], and no data on spine energy distribution.

A synaptic connection between excitatory neurons, which are majority in the cortex [38], can potentially be generated in that cortical region where axonal and dendritic trees spatially overlap [71]. However, a physical vicinity of axons and dendrites may not be sufficient for the appearance of a spine in this location [72], which suggests an additional factor of possibly stochastic nature involved [69]. It is assumed here that this factor is associated with energy. Specifically, we require that a metabolic energy allocated to a spine must be above a certain threshold to form a stable spine (or equivalently that potential spine volume must be large enough). This requirement relates to the empirical fact that physiological processes need a minimal amount of energy to be activated [73], which seems to apply to dendritic spines, since they disappear during prolonged severe ischemia [74] and during excessive cooling of the tissue [75]. Thus, the average probability of finding a spine at some location is equal to the product of two average probabilities: that axons and dendrites are present there, and that a potential spine is larger than a certain threshold. On the other hand, based on the concept of geometric probability, the probability of finding a spine in the cortex is approximately equal to the fractional cortical volume occupied by spines, which is denoted as s. Mathematically, this means:

$$s = Pxy, \tag{2}$$

where the parameters x and y denote fractional volumes of axons and dendrites in the cortex or probabilities of their occurrence (i.e. $0 < x, y < 1$). The product xy is the average probability that both axon and dendrite are present in a small cortical space. The symbol P is the conditional probability that a spine has volume u that is greater than the threshold θ. Formally, this

probability is defined as

$$P = \int_{\theta}^{\infty} H(u)du, \tag{3}$$

where $H(u)$ is the distribution (density of probability) of spine volumes u. One can view P as a conditional probability of spine formation. We consider five different types of volume distribution functions $H(u)$, for which we obtain different forms of the probability $P(\bar{u})$ as a function of average spine volume $\bar{u}$ (see below).

Distributions of spine sizes. Empirical data show that spines can have widely different sizes, from very small $\sim 0.01\ \mu m^3$ to quite large $\sim 1.3\ \mu m^3$ [41, 76]. The distribution of their sizes has been fitted by two distinct functions with different asymptotic properties, either by gamma function with short-tail [41], or by log-normal with heavy-tail [69]. This suggests that there could also be other distributions, which are statistically indistinguishable from the above, that would fit the data equally well. For this reason and for a larger generality we consider five different distributions $H(u)$ of spine volumes: three with short-tail and two with heavy-tail. For each distribution we provide explicit forms of the conditional probability P in terms of the average spine volume $\bar{u}$, which is defined as

$$\bar{u} = \int_{0}^{\infty} H(u)udu. \tag{4}$$

Exponential distribution.
This type of spine volume distribution has the form:

$$H(u) = \alpha e^{-\alpha u} \tag{5}$$

for $u \geq 0$, where α is some positive constant. The average spine volume is $\bar{u} = 1/\alpha$. The conditional probability P (defined in Eq 3) that a spine is greater than the threshold θ is

$$P(\bar{u}) = e^{-\theta/\bar{u}}, \tag{6}$$

i.e. it can be expressed as a function of $\bar{u}$. The latter feature applies to all size distributions considered in this paper (see below). For $\bar{u}/\theta \ll 1$ the probability $P(\bar{u}) \ll 1$, whereas for $\bar{u}/\theta \gg 1$ we have $P(\bar{u}) \approx 1$.

Gamma distribution.
The distribution of spine volume H is:

$$H(u) = \frac{\alpha^{n+1}}{n!} u^n e^{-\alpha u} \tag{7}$$

for $u \geq 0$, where α is some positive constant. The average spine volume is $\bar{u} = (n+1)/\alpha$. The probability $P = \Gamma(n+1, (n+1)\theta\bar{u})$, where Γ is the standard Gamma function. In the paper we consider two special cases, with $n = 1$ and $n = 2$, for which the probability P takes the following forms:

$$P(\bar{u}) = \left(1 + 2\frac{\theta}{\bar{u}}\right) e^{-2\theta/\bar{u}} \tag{8}$$

for $n = 1$, and

$$P(\bar{u}) = \left[1 + 3\frac{\theta}{\bar{u}} + \frac{9}{2}\left(\frac{\theta}{\bar{u}}\right)^2\right] e^{-3\theta/\bar{u}} \tag{9}$$

for $n = 2$.

Rayleigh distribution.

The distribution of spine volume is given by

$$H(u) = \frac{u}{\sigma^2} e^{-u^2/(2\sigma^2)} \tag{10}$$

for $u \geq 0$. The average spine volume is $\bar{u} = \sqrt{\frac{\pi}{2}}\sigma$. The probability P that spine is larger than the threshold θ is

$$P(\bar{u}) = e^{-\frac{\pi}{4}(\theta/\bar{u})^2}. \tag{11}$$

Log-logistic distribution.
This type of distribution has a heavy tail and is represented by

$$H(u) = \frac{\beta}{\alpha} \frac{(u/\alpha)^{\beta-1}}{[1+(u/\alpha)^\beta]^2} \tag{12}$$

for $u \geq 0$, where α is a positive constant and $\beta > 1$. Note that $H(u)$ decays as a power law for asymptotically large u. The average spine volume is $\bar{u} = \alpha\pi/(\beta \sin(\pi/\beta))$. The probability P in terms of $\bar{u}$ is given by

$$P(\bar{u}) = \frac{\bar{u}^\beta}{\bar{u}^\beta + \tilde{\theta}^\beta}, \tag{13}$$

where $\tilde{\theta}$ is the renormalized threshold, i.e. $\tilde{\theta} = \theta \frac{(\pi/\beta)}{\sin(\pi/\beta)}$. Eq (13) is known as Hill equation and is often used in biochemistry when there are cooperative phenomena between different molecules. Note that for sufficiently large exponent β, the probability $P \ll 1$ if $\bar{u} < \tilde{\theta}$, and $P \sim 1$ if $\bar{u} > \tilde{\theta}$.

Log-normal distribution.
The distribution of spine volume in this case also has a heavy tail, and it is given by

$$H(u) = \frac{1}{\sqrt{2\pi}\sigma u} \exp\left[-\frac{(\ln u - \mu)^2}{2\sigma^2}\right], \tag{14}$$

where μ and σ are some parameters ($\sigma > 0$). The average spine volume $\bar{u}$ is $\bar{u} = \exp(\mu + \sigma^2/2)$. The probability that a spine has larger volume than the threshold θ is

$$P(\bar{u}) = \frac{1}{2}\left[1 - \text{erf}\left(\frac{\ln(\theta/\bar{u}) + \sigma^2/2}{\sqrt{2}\sigma}\right)\right], \tag{15}$$

where erf(...) is the standard error function. Note that for $\sigma \ll 1$, we have $P \sim 1$ if $\bar{u}/\theta \gg 1$ and $P \ll 1$ if $\bar{u}/\theta \ll 1$.

Model of glia and capillary fractional volumes. The model of glia and capillary fractions presented below relies on empirical evidence that cortical neurons with their synapses are spatially coupled to glia (astrocytes) and microvasculature. Specifically, it was shown that neuron density for mouse cortex and macaque monkey visual cortex correlate with vascular length density [29, 30]. The changes in astrocyte density are to some extent related to changes in capillary density across layers of mouse somatosensory cortex [31] (see below). Moreover, developmental data for cat visual cortex show a strong spatio-temporal coupling between capillary length density and synaptic density [77].

Extended branching processes of astrocytes resemble dendritic trees of neurons [78]. The endings of these processes physically connect with spines by wrapping around their surface to provide spines with metabolic substrates and glutamate from capillaries, and to remove waste

products [78]. The transport of metabolites to and from spines along astrocytes should be effective, i.e. sufficiently fast and the least energy consuming, otherwise spines and thus local neural circuits would not get enough energy on time and as a result would underperform their functions. (Although glia use much less energy than neurons [21], they nevertheless should minimize their metabolic needs for the overall brain efficiency). This suggests that the total length of astrocyte processes should be as small as possible. Consequently, we can treat an astrocyte as a minimal spanning tree along its target points, i.e., spines. It can be shown mathematically that in a minimal tree formalism, the total length of the tree connecting n target points or branch points scales asymptotically as $n^{2/3}$ [79, 80]. The important point is that this result applies universally to any transportation network that works efficiently. Additionally, because of the physical units consistency, the total length of the tree should scale with enclosing volume V as $V^{1/3}$. Thus, the total length L of processes of a single astrocyte connecting N_s spines should be minimized when

$$L = bN_s^{2/3}V^{1/3}, \tag{16}$$

where b is some constant. It can be shown theoretically under general conditions that $b = (3/(4\pi))^{1/3}$ [5]. This value was also found empirically for neural dendritic trees [5], and because of the structural similarity between branching patterns of astrocytes and dendrites, this particular value of b is also adopted here. The parameter V in Eq (16) is the cortical volume enclosing a single astrocyte and N_s spines. This "domain volume" is defined by three-dimensional boundaries of an astrocyte, and it is much bigger than the actual volume of an astrocyte because it includes also other cortical components (spines, dendrites, axons, etc) contained within these boundaries. The critical feature of astrocyte domains is that neighboring astrocytes essentially do not overlap, which means that each domain contains only one astrocyte cell that influences synaptic spines only from that particular domain. This property of astrocytes spatial arrangement is called domain organization ([78, 81]).

The main contribution to astrocyte volume comes from astrocyte free processes (astrocyte soma and astrocyte perivascular sheath constitute only 28% and 7% of the total astrocyte volume; [67]). Assuming a cylindrical geometry for these extended processes, the total volume of an astrocyte V_{as} can be approximated as $V_{as} = (\pi/4)Ld_{as}^2$, where d_{as} is the average diameter of all free processes. The value of d_{as} can be estimated based on data for volume ($V_{pr} = 350 \, \mu m^3$) and surface area ($S_{pr} = 1650 \, \mu m^2$) of astrocyte processes (without soma) in the cat sensorimotor cortex [59]. Using a familiar formula $d_{as} = 4V_{pr}/S_{pr}$, we obtain $d_{as} = 0.85 \, \mu m$. One can expect that the value of d_{as} only very weakly depends on brain size, as it is the case for diameters of the thickest processes, which are 2.2 μm for mouse, and 2.9 μm for human [82], despite four orders of magnitude difference in brain volumes of these mammals (e.g. [22]). For that reason, the value $d_{as} = 0.85 \, \mu m$ is kept constant for all computations performed in this study, and it is the only parameter that is fixed in the model.

Because of the astrocyte domains segregation, the volume fraction of astrocytes can be defined as $g = V_{as}/V$, which combined with Eq (16) yields

$$g = a\rho_s^{2/3} = \frac{as^{2/3}}{\bar{u}^{2/3}}, \tag{17}$$

where $a = (\pi/4)bd_{as}^2 = 0.352 \mu m^2$, spine density $\rho_s = N_s/V$, and in the last equality we used the fact that density ρ_s, spine proportion s, and average spine volume $\bar{u}$ are related by

$$s = \rho_s \bar{u}. \tag{18}$$

The spatial separation between capillaries and spines, and between capillaries and astrocytes is relatively small, which presumably ensures a high efficiency of energy delivery. For example, a typical distance between capillaries and spines in mouse cortex is roughly 13 μm [74]. Many astrocyte processes are either in the vicinity or directly touch capillaries [78]. Even astrocyte somata is close to microvasculature, with mean spacing between them 6–10 μm in mouse somatosensory cortex, which at some locations can be down to $\sim$ 1 μm [31]. For a comparison, an intercapillary distance is generally much larger: 32–43 μm for mouse cortex [83], and 58 μm for human cortex [84]. These data suggest that capillaries cluster in those cortical places where there are high densities of both astrocytes and spines. Mathematically, this means that the probability of finding a capillary at some location (or equivalently, fraction of capillary volume c) is proportional to probability of finding both an astrocyte (equal to volume fraction g) and a spine (equal to volume fraction s). The simplest form of such a probabilistic relationship is their product, i.e.

$$c = gs. \tag{19}$$

There is some additional empirical support for that "product formula" based on a laminar distribution of microvasculature and synapses both for rodents and for primates. For mouse somatosensory cortex, capillary fraction and astrocyte density correlate across cortical layers [31], but their relationship is clearly nonlinear, as local peaks in these two variables often do not exactly match (compare Fig. 1 in [31]). It seems that inclusion of spine density in that relationship should improve the correlation with changes in capillary fraction variability. Specifically, capillary fraction exhibits a peak in cortical somatosensory layer 1, which is however absent in the corresponding astrocyte density [31], but it correlates well with the fact that the density of asymmetric synapses (mostly spines) is the largest in the layer 1 of mouse somatosensory cortex [85].

For primate visual cortex, capillary length density is the largest in the middle layers 4 and 2/3, and the smallest in layers 1 and 5/6 [30, 86], which is similar to the laminar distribution of synaptic density, although with some fluctuations [87, 88]. Taken together, these data suggest that microvasculature is correlated with both synapses and astrocytes in the cortical gray matter.

Capillary fraction c in Eq (19) can be expressed in terms of spine parameters using Eq (17) for g, with the result

$$c = \frac{as^{5/3}}{\bar{u}^{2/3}}. \tag{20}$$

Note, that because $s \sim g^{3/2}$, we have equivalently that $c \sim g^{5/2}$, which indicates a strong nonlinear dependence between capillary and astrocyte volume fractions, and suggests that generally one can expect $c/g \ll 1$.

The fitness functions. We consider three different classes of fitness functions. The first corresponds to the principle of neural "wire minimization" and the second to the proposed here "spine economical maximization". The third class is a combination of the first two.

<u>Wire minimization principle.</u>

The most general form of the fitness function F_w (benefit-cost or Lagrange function) for wire minimization takes the form:

$$F_w = \frac{rx + y}{\bar{u}^{\gamma_1}} + \lambda_1 (x + y + s + g + c - 1), \tag{21}$$

where the exponent $\gamma_1 > 0$ corresponds to specific characteristics of neuronal wire one wants to minimize (wire length, its surface area, its volume or conduction delays; see below). The free

parameter r is a measure of the asymmetry between axons and dendrites. The parameter λ_1 is the Lagrange multiplier associated with the volume normalization constraint: $x + y + s + g + c = 1$, i.e., fractional volumes of all considered cortical components must sum up to unity. The fitness function $F_w(x, y, \bar{u})$ is the function of the three independent variables x, y, and $\bar{u}$, because the fractions s, g, and c depend on these variables (see Eqs (2), (17) and (20)).

The form of the benefit-cost function in Eq (21) can be justified by taking neural wire length minimization as an example. The other cases can be analyzed analogously. The total axonal volume in the cortex is $V_a = (\pi/4)L_a d_a^2$, where L_a is the total axon length in the cortex and d_a is the average axon diameter. Similarly, for the total dendrite volume we have $V_d = (\pi/4)L_d d_d^2$, where L_d is the total dendrite length and d_d is its diameter. Now, consider the fitness function F_{w0} as a density of combined lengths of axons and dendrites with some proportion coefficient r_0:

$$F_{w0} \sim \frac{r_0 L_a + L_d}{V},\qquad(22)$$

where V is the volume of cortical gray matter. If we represent L_a and L_d in terms of V_a and V_d, and denote the fractional volumes of axons and dendrites respectively as $x = V_a/V$ and $y = V_d/V$, then we obtain that

$$F_{w0} \sim \frac{(d_d/d_a)^2 r_0 x + y}{d_d^2}.\qquad(23)$$

The empirical data indicate that average spine heads (postsynaptic density PSD) and dendrites have diameters of the same order of magnitude (fraction of micron), which do not seem to depend significantly on brain size [14]. This suggests that these two diameters can be mutually coupled, which implies that one can assume that $d_d^2 \sim \bar{u}^{\gamma_1}$, where the exponent $\gamma_1 \approx 2/3$ (the bulk of the spine has a spherical shape). Moreover, if we denote $r = r_0(d_d/d_a)^2$, then we obtain Eq (21) for the full (with the Lagrange multiplier term) fitness function.

A similar analysis performed for wire surface minimization and wire volume minimization yields the same formula but with different γ_1, respectively 1/3 and 0. For the case of conduction delays minimization, one can define a similar fitness function to F_{w0} in Eq (22) with the substitutions $L_a \mapsto L_a/\sqrt{d_a}$ and $L_d \mapsto L_d/\sqrt{d_d}$, which approximately correspond to temporal delays along axons and dendrites, as the conduction velocity is proportional to a square root of unmyelinated wire diameter [48]. Performing the analysis analogously, one obtains Eq (21) with $\gamma_1 = 5/6$ and $r = r_0(d_d/d_a)^{5/2}$.

Spine economical maximization principle.

The most general form of the fitness function F_s for spine proportion economical maximization takes the form:

$$F_s = \frac{s}{\bar{u}^{\gamma_2}} + \lambda_2 (x + y + s + g + c - 1),\qquad(24)$$

where the exponent $\gamma_2 > 0$ characterizes the influence of spine size on the maximization process (γ_2 here is generally numerically different than γ_1 in Eq (21)), and the parameter λ_2 is the Lagrange multiplier as before. This proposition can be justified as follows. The analysis of experimental data on the developing cerebral cortex in several mammals indicate that the ratio of cerebral metabolic rate CMR (the rate of glucose consumption per cortical volume) and synaptic density ρ_s is approximately conserved from birth until adulthood for a given region of the cortex, despite large variabilities in CMR and ρ_s [27]. This means that CMR/$\rho_s \approx$ const. Synaptic density is comprised mostly of the density of spines (synapses in the cerebral cortex are in

80–90% excitatory, most of which are axo-spinal [18], and this percentage does not depend on brain size; [14]), which is related to spine fractional volume s via the formula $s = \rho_s \bar{u}$. This implies that the ratio $CMR\bar{u}/s$ is roughly conserved during development. The product in the nominator can be identified as an average metabolic energy per spine, which should be proportional to spine volume at some power $\gamma_2 \geq 0$, i.e. $CMR\bar{u} \sim \bar{u}^{\gamma_2}$, because spine energy is associated mainly with the activity of Na/K-ATP pumps located on spine surface area [21, 89]. Thus, we obtain that the ratio $s/\bar{u}^{\gamma_2}$ should be developmentally approximately constant for a given cortical area, which indicates that this ratio is probably important for cortical functioning. Consequently, it is assumed here that there has been an evolutionary pressure on increasing the proportion of spines in the cortex that would consume the least energy or take the smallest size (spines are energy demanding [25–27]). These considerations lead to the maximization of the benefit-cost function given by Eq (24).

  Combined wire minimization and spine economical maximization as a meta principle.

  The simplest fitness function F that generalizes both notions of wire minimization and spine maximization, and includes them simultaneously is a linear combination of their corresponding primary fitness functions F_w and F_s. If part of F associated with F_w is to be minimized, and part of F related to F_s is to be maximized, then we must include F_w and F_s with opposite signs. Therefore, we define the meta fitness function F, which we want to minimize, as

$$F = f\,F_w - (1-f)F_s, \tag{25}$$

where f is the parameter controlling relative contributions of wire minimization and spine economy maximization Lagrangians, with the condition $0 \leq f \leq 1$. As we gradually decrease f from 1 to 0, then the meta fitness function F changes its character form dominated by wire minimization to dominated by spine economy maximization. The case $f = 1/2$ corresponds to a symmetric situation when both wire min and spine max rules are equally important. Note that minimization of $(-F_s)$ is mathematically equivalent to maximization of F_s. Eq (1) in the Results section is obtained after substitution of Eqs (21) and (24) for F_w and F_s in Eq (25).

  Optimization of the fitness functions. Optimal fractional volumes of axons x, dendrites y, spines s, glia/astrocytes g, capillaries c, and optimal average spine volume $\bar{u}$ are found by taking partial derivatives of F, i.e., $\partial F/\partial x = \partial F/\partial y = \partial F/\partial \bar{u} = \partial F/\partial \lambda = 0$. As a result we obtain a system of three basic equations (details are provided in Supp. Information S1 Text):

$$(1-f)s(y-x) + f\bar{u}^{\gamma_2 - \gamma_1}\left[xy(1-r) + (y-rx)\left[s + \frac{g}{3}(2+5s)\right]\right] = 0, \tag{26}$$

$$\left[(1-f)s\bar{u}^{\gamma_1} + f\bar{u}^{\gamma_2}\left(s + \frac{2}{3}g + \frac{5}{3}c\right)\right]\frac{y\bar{u}}{P}\frac{\partial P}{\partial \bar{u}} =$$
$$\left(y + s + \frac{2}{3}g + \frac{5}{3}c\right)[(1-f)\gamma_2 s\bar{u}^{\gamma_1} - f\gamma_1(y+rx)\bar{u}^{\gamma_2}] \tag{27}$$
$$+ \frac{2}{3}(g+c)[fy\bar{u}^{\gamma_2} - (1-f)s\bar{u}^{\gamma_1}],$$

and

$$x + y + s + g + c = 1. \tag{28}$$

In the case of pure wire minimization principle, i.e. when $f = 1$, the above system reduces to the

following equations (with explicit dependencies of s, g, and c on x, y, and P:

$$(rx - y)\left[P + \frac{a}{3}\left(\frac{P^2}{xy\bar{u}^2}\right)^{1/3}(2 + 5Pxy)\right] = 1 - r, \tag{29}$$

$$\frac{2}{3}aPx^{2/3}y(1 + Pxy) - \gamma_1(rx + y)P^{1/3}\left[\bar{u}^{2/3}y^{1/3}(1 + Px) + \frac{a}{3}(Px)^{2/3}(2 + 5Pxy)\right]$$
$$= \bar{u}\frac{\partial P}{\partial \bar{u}}\left[P^{1/3}\bar{u}^{2/3}xy^{4/3} + \frac{a}{3}x^{2/3}y(2 + 5Pxy)\right], \tag{30}$$

and

$$x + y + Pxy + \frac{a(Pxy)^{2/3}}{\bar{u}^{2/3}} + \frac{a(Pxy)^{5/3}}{\bar{u}^{2/3}} = 1. \tag{31}$$

In the case of pure spine economical maximization principle, i.e. when $f = 0$, the system of Eqs (26–28) reduces to two equations:

$$\bar{u}^{2/3}\frac{\partial P}{\partial \bar{u}} = \frac{P}{\bar{u}}\left(\gamma_2\bar{u}^{2/3}(1 + Px) + \frac{a}{3}P^{2/3}x^{1/3}[2(\gamma_2 - 1) + (5\gamma_2 - 2)Px^2]\right) \tag{32}$$

and

$$2x + Px^2 + \frac{a(Px^2)^{2/3}}{\bar{u}^{2/3}} + \frac{a(Px^2)^{5/3}}{\bar{u}^{2/3}} = 1, \tag{33}$$

since in this case $x = y$.

The above equations are solved numerically for each distribution of spine volumes, using standard techniques [90]. In the case of pure wire minimization, the optimal solution corresponds to a local minimum of F_w, whereas for pure spine economy maximization the optimal solution is associated with a local maximum of F_s (see S1 Text). For a mixed case with $0 < f < 1$, the optimal solution is a local minimum of F (S1 Text).

Comparison of the theoretical results to the data. The optimal theoretical fractional volumes were compared to the empirical fractional volumes in the cerebral cortex using two related measures of similarity: Euclidean distance (ED) and Mahalanobis distance (MD). The major difference between these two measures is in their treatment of variance in the data. ED measures a distance between theoretical points and mean values of data points ignoring their variance, whereas MD measures such a normalized distance including standard deviations of data points [91]. Thus MD is more general than ED. The best similarity with the data is achieved for minimal values of MD and ED.

ED distance between theoretical and experimental points is defined as:

$$\text{ED} = \sqrt{\sum_{i=1}^{5}(x_i - x_{ex,i})^2}, \tag{34}$$

where x_i and $x_{ex,i}$ are respectively theoretical and mean empirical values of fractional volumes of axons, dendrites, spines, glia/astrocytes, and capillaries in the cortex (experimental data correspond to the next-to-last line in Table 1).

MD distance between theoretical and experimental points is defined as [91]:

$$\text{MD} = \sqrt{\sum_{i=1}^{5}\left(\frac{x_i - x_{ex,i}}{sd_{ex,i}}\right)^2}, \tag{35}$$

where x_i and $x_{ex,i}$ are the same as in Eq (34), and $sd_{ex,i}$ denotes the standard deviation associated with each data point (the next-to-last line in Table 1). It is easy to see that MD defined above is simply a variance-normalized ED distance. In a special case when all standard deviations $sd_{ex,i}$ are equal to unity, MD reduces to ED.

Supporting Information

S1 Text. This file contains Supporting Figure A and Supporting Tables A-E. It also provides some details of the derivations, and proofs of minimum for F_w and F, and proof of maximum for F_s.
(PDF)

Author Contributions

Conceived and designed the experiments: JK. Performed the experiments: JK. Analyzed the data: JK. Contributed reagents/materials/analysis tools: JK. Wrote the paper: JK.

References

1. Iadecola C (2004) Neurovascular regulation in the normal brain and in Alzheimer's disease. *Nat. Rev. Neurosci*. 5: 347–360. PMID: 15100718

2. Attwell D, Buchan AN, Charpak S, Lauritzen M, MacVicar BA, Newman EA (2010) Glial and neuronal control of brain blood flow. *Nature* 468: 232–243. doi: 10.1038/nature09613 PMID: 21068832

3. Wen Q, Stepanyants A, Elston G, Grosberg AY, Chklovskii DB (2009) Maximization of the connectivity repertoire as a statistical principle governing the shapes of dendritic arbors. *Proc. Natl. Acad. Sci. USA* 106: 12536–12541. doi: 10.1073/pnas.0901530106 PMID: 19622738

4. Snider J, Pillai A, Stevens CF (2010) A universal property of axonal and dendritic arbors. *Neuron* 66: 45–56. doi: 10.1016/j.neuron.2010.02.013 PMID: 20399728

5. Cuntz H, Mathy A, Hausser M (2012) A scaling law derived from optimal dendritic wiring. *Proc. Natl. Acad. Sci. USA* 109: 11014–11018. doi: 10.1073/pnas.1200430109 PMID: 22715290

6. Karbowski J (2011) Scaling of brain metabolism and blood flow in relation to capillary and neural scaling. *PLoS ONE* 6: e26709. doi: 10.1371/journal.pone.0026709 PMID: 22053202

7. Cherniak C (1994) Component placement optimization in the brain. *J. Neuroscience* 14: 2418–2427. PMID: 8158278

8. Chklovskii DB, Schikorski T, Stevens CF (2002) Wiring optimization in cortical circuits. *Neuron* 34: 341–347. doi: 10.1016/S0896-6273(02)00679-7 PMID: 11988166

9. Wen Q, Chklovskii DB (2005) Segregation of the brain into gray and white matter: A design minimizing conduction delays. *PLoS Comput. Biol*. 1: e78. doi: 10.1371/journal.pcbi.0010078 PMID: 16389299

10. Klyachko VA, Stevens CF (2003) Connectivity optimization and the positioning of cortical areas. *Proc. Natl. Acad. Sci. USA* 100: 7937–7941. doi: 10.1073/pnas.0932745100 PMID: 12796510

11. Budd JML, Kovacs K, Ferecsko AS, Buzas P, Eysel UT, Kisvarday ZF (2010) Neocortical axon arbors trade-off material and conduction delay conservation. *PLoS Comput. Biol*. 6: e1000711. doi: 10.1371/journal.pcbi.1000711 PMID: 20300651

12. Budd JML, Kisvarday ZF (2012) Communication and wiring in the cortical connectome. *Front. Neuroanat*. 6: 42. doi: 10.3389/fnana.2012.00042 PMID: 23087619

13. Bullmore E, Sporns O (2012) The economy of brain network organization. *Nat. Rev. Neurosci*. 13: 336–349. PMID: 22498897

14. Karbowski J (2014) Constancy and trade-offs in the neuroanatomical and metabolic design of the cerebral cortex. *Front. Neural Circuits* 8: 9. doi: 10.3389/fncir.2014.00009 PMID: 24574975

15. Kaiser M, Hilgetag CC (2006) Nonoptimal component placement, but short processing paths, due to long-distance projections in neural systems. *PLoS Comput. Biol*. 2: e95. doi: 10.1371/journal.pcbi.0020095 PMID: 16848638

16. Chen Y, Wang S, Hilgetag CC, Zhou C (2013) Trade-off between multiple constraints enables simultaneous formation of modules and hubs in neural systems. *PLoS Comput. Biol*. 9: e1002937. doi: 10.1371/journal.pcbi.1002937 PMID: 23505352

17. Cherniak C, Mokhtarzada Z, Rodriguez-Esteban R, Changizi K (2004) Global optimization of cerebral cortex layout. *Proc. Natl. Acad. Sci. USA* 101: 1081–1086. doi: 10.1073/pnas.0305212101 PMID: 14722353

18. Zecevic N, Rakic P (1991) Synaptogenesis in monkey somatosensory cortex. *Cereb. Cortex* 1: 510–523. doi: 10.1093/cercor/1.6.510 PMID: 1822755

19. Kasai H, Matsuzaki M, Noguchi J, Yasumatsu N, Nakahara H (2003) Structure-stability-function relationships of dendritic spines. *Trends Neurosci*. 26: 360–368. doi: 10.1016/S0166-2236(03)00162-0 PMID: 12850432

20. Aiello LC, Wheeler P (1995) The expensive-tissue hypothesis: The brain and the digestive-system in human and primate evolution. *Curr. Anthropology* 36: 199–221. doi: 10.1086/204350

21. Attwell D, Laughlin SB (2001) An energy budget for signaling in the gray matter of the brain. *J. Cereb. Blood Flow Metabol*. 21: 1133–1145. doi: 10.1097/00004647-200110000-00001

22. Karbowski J (2007) Global and regional brain metabolic scaling and its functional consequences. *BMC Biology* 5: 18. doi: 10.1186/1741-7007-5-18 PMID: 17488526

23. Levy WB, Baxter RA (1996) Energy efficient neural codes. *Neural Computation* 8: 531–543. doi: 10.1162/neco.1996.8.3.531 PMID: 8868566

24. Laughlin SB, de Ruyter van Steveninck RR, Anderson JC (1998) The metabolic cost of neural information. *Nature Neurosci*. 1: 36–40. doi: 10.1038/236 PMID: 10195106

25. Alle H, Roth A, Geiger JRP (2009) Energy-efficient action potentials in hippocampal mossy fibers. *Science* 325: 1405–1408. doi: 10.1126/science.1174331 PMID: 19745156

26. Harris JJ, Jolivet R, Attwell D (2012) Synaptic energy use and supply. *Neuron* 75: 762–777. doi: 10.1016/j.neuron.2012.08.019 PMID: 22958818

27. Karbowski J (2012) Approximate invariance of metabolic energy per synapse during development in mammalian brains. *PLoS ONE* 7: e33425. doi: 10.1371/journal.pone.0033425 PMID: 22479396

28. Chugani HT (1998) A critical period of brain development: Studies of cerebral glucose utilization with PET. *Preventive Medicine* 27: 184–188. doi: 10.1006/pmed.1998.0274 PMID: 9578992

29. Tsai PS, Kaufhold J, Blinder P, Friedman B, Drew PJ et al (2009) Correlations of neuronal and microvascular densities in murine cortex revealed by direct counting and colocalization of nuclei and vessels. *J. Neurosci*. 29: 14553–14570. doi: 10.1523/JNEUROSCI.3287-09.2009 PMID: 19923289

30. Weber B, Keller AL, Reichold J, Logothetis NK (2008) The microvascular system of the striate and extrastriate visual cortex of the macaque. *Cereb. Cortex* 18: 2318–2330. doi: 10.1093/cercor/bhm259 PMID: 18222935

31. McCaslin AFH, Chen BR, Radosevich AJ, Cauli B, Hillman EMC (2011) In vivo 3D morphology of astrocyte-vasculature interactions in the somatosensory cortex: implications for neurovascular coupling. *J. Cereb. Blood Flow Metabol*. 31: 795–806. doi: 10.1038/jcbfm.2010.204

32. Montague PR (1996) The resource consumption principle: attention and memory in volumes of neural tissue. *Proc. Natl. Acad. Sci. USA* 93: 3619–3623. doi: 10.1073/pnas.93.8.3619 PMID: 8622985

33. Kaas JH (2000) Why is brain size so important: Design problems and solutions as neocortex gets bigger or smaller. *Brain Mind* 1: 7–23. doi: 10.1023/A:1010028405318

34. Bassett DS, Greenfield DL, Meyer-Lindenberg A, Weinberger DR, Moore SW, Bullmore ET (2010) Efficient physical embedding of topologically complex information processing networks in brains and computer circuits. *PLoS Comput. Biol*. 6: e1000748. doi: 10.1371/journal.pcbi.1000748 PMID: 20421990

35. Parker GA, Maynard Smith J (1990) Optimality theory in evolutionary biology. *Nature* 348: 27–33. doi: 10.1038/348027a0

36. Alexander RM (1996) *Optima for Animals*. Princeton, NJ: Princeton Univ. Press.

37. Striedter GF (2005) *Principles of Brain Evolution*. Sunderland, MA: Sinauer Assoc.

38. Braitenberg V, Schüz A (1998) *Cortex: Statistics and Geometry of Neuronal Connectivity*. Berlin: Springer.

39. Herculano-Houzel S, Mota B, Wong P, Kaas JH (2010) Connectivity-driven white matter scaling and folding in primate cerebral cortex. *Proc. Natl. Acad. Sci. USA* 107: 19008–19013. doi: 10.1073/pnas.1012590107 PMID: 20956290

40. Mayhew TM, Mwamengele GLM, Dantzer V (1996) Stereological and allometric studies on mammalian cerebral cortex with implications for medical brain imaging. *J. Anat*. 189: 177–184. PMID: 8771409

41. Benavides-Piccione R, Fernaud-Espinosa I, Robles V, Yuste R, DeFelipe J (2013) Age-based comparison of human dendritic spine structure using complete three-dimensional reconstructions. *Cerebral Cortex* 23: 1798–1810. doi: 10.1093/cercor/bhs154 PMID: 22710613

42. Villalba RM, Smith Y (2010) Striatal spine plasticity in Parkinson's disease. *Front. Neuroanat*. 4: 133. doi: 10.3389/fnana.2010.00133 PMID: 21179580

43. Stevens CF (2011) Brain organization: Wiring economy works for the large and small. *Curr. Biol*. 22: R24. doi: 10.1016/j.cub.2011.11.036

44. Bonhoeffer T, Yuste R (2002) Spine motility: phenomenology, mechanisms, and function. *Neuron* 35: 1019–1027. doi: 10.1016/S0896-6273(02)00906-6 PMID: 12354393

45. Holtmaat AJ, Trachtenberg JT, Wilbrecht L, Shepherd GM, Zhang X, et al (2005) Transient and persistent dendritic spines in the neocortex in vivo. *Neuron* 45: 279–291. doi: 10.1016/j.neuron.2005.01.003 PMID: 15664179

46. Statman A, Kaufman M, Minerbi A, Ziv NE, Brenner N (2014) Synaptic size dynamics as an effective stochastic process. *PLoS Comput. Biol*. 10: e1003846. doi: 10.1371/journal.pcbi.1003846 PMID: 25275505

47. Meyer D, Bonhoeffer T, Scheuss V (2014) Balance and stability of synaptic structures during synaptic plasticity. *Neuron* 82: 430–443. doi: 10.1016/j.neuron.2014.02.031 PMID: 24742464

48. Hursh JB (1939) Conduction velocity and diameter of nerve fibers. *Amer. J. Physiol*. 127: 131–139.

49. Wang SSH, Shultz JR, Burish MJ, Harrison KH, Hof PR, et al (2008) Functional trade-offs in white matter axonal scaling. *J. Neurosci*. 28: 4047–4056. doi: 10.1523/JNEUROSCI.5559-05.2008 PMID: 18400904

50. Perez-Escudero A, de Polavieja GG (2007) Optimally wired subnetwork determines neuroanatomy of Caenorhabditis elegans. *Proc. Natl. Acad. Sci. USA* 104: 17180–17185. doi: 10.1073/pnas.0703183104 PMID: 17942697

51. Karbowski J (2001) Optimal wiring principle and plateaus in the degree of separation for cortical neurons. *Phys. Rev. Lett*. 86: 3674–3677. doi: 10.1103/PhysRevLett.86.3674 PMID: 11328051

52. Stepanyants A, Martinez LM, Ferecsko AS, Kisvarday ZF (2009) The fractions of short- and long-range connections in the visual cortex. *Proc. Natl. Acad. Sci. USA* 106: 3555–3560. doi: 10.1073/pnas.0810390106 PMID: 19221032

53. Chklovskii DB, Mel BW, Svoboda K (2004) Cortical rewiring and information storage. *Nature* 431: 782–788. doi: 10.1038/nature03012 PMID: 15483599

54. Landau LD, Lifshitz EM (1960) *Mechanics*. Pergamon Press: New York.

55. Mishchenko Y, Hu T, Spacek J, Mendenhall J, Harris KM, Chklovskii DB (2010) Ultrastructural analysis of hippocampal neuropil from the connectomics perspective. *Neuron* 67: 1009–1020. doi: 10.1016/j.neuron.2010.08.014 PMID: 20869597

56. Bar TH (1980) The vascular system of the cerebral cortex. *Adv. Anat. Embryol. Cell Biol*. 59: 71–84.

57. Schmolke C, Schleicher A (1989) Structural inhomogeneity in the neuropil of lamina II/III in rabbit visual cortex. *Exp. Brain Res*. 77: 39–47. doi: 10.1007/BF00250565 PMID: 2792268

58. Mainen Z, Sejnowski T (1996) Influence of dendritic structure on firing patterns in model neocortical neurons. *Nature* 382: 363–366. doi: 10.1038/382363a0 PMID: 8684467

59. Williams V, Grossman RG, Edmunds SM (1980) Volume and surface area estimates of astrocytes in the sensorimotor cortex of the cat. *Neuroscience* 5: 1151–1159. doi: 10.1016/0306-4522(80)90194-3 PMID: 7402464

60. Pawlik G, Rackl A, Bing RS (1981) Quantitative capillary topography and blood flow in the cerebral cortex of cat: an in vivo microscopic study. *Brain Res*. 208: 35–58. doi: 10.1016/0006-8993(81)90619-3 PMID: 7470927

61. Christensen JR, Larsen KB, Lisanby SH, Scalia J, Arango V, et al (2007) Neocortical and hippocampal neuron and glial cell numbers in the rhesus monkey. *Anatomical Record* 290: 330–340. doi: 10.1002/ar.20504

62. Hao J, Papp PR, Leffler AE, Leffler SR, Janssen WG, et al (2006) Estrogen alters spine number and morphology in prefrontal cortex of aged female rhesus monkeys. *J. Neurosci*. 26: 2571–2578. doi: 10.1523/JNEUROSCI.3440-05.2006 PMID: 16510735

63. Escobar G, Fares T, Stepanyants A (2008) Structural plasticity of circuits in cortical neuropil. *J. Neurosci*. 28: 8477–8488. doi: 10.1523/JNEUROSCI.2046-08.2008 PMID: 18716206

64. Medalla M, Barbas H (2009) Synapses with inhibitory neurons differentiate anterior cingulate from dorsolateral prefrontal pathways associated with cognitive control. *Neuron* 61: 609–620. doi: 10.1016/j.neuron.2009.01.006 PMID: 19249280

65. Dumitriu D, Hao J, Hara Y, Kaufmann J, Janssen WG, et al (2010) Selective changes in thin spine density and morphology in monkey prefrontal cortex correlate with aging-related cognitive impairment. *J. Neurosci*. 30: 7507–7515. doi: 10.1523/JNEUROSCI.6410-09.2010 PMID: 20519525

66. Alonso-Nanclares L, Gonzalez-Soriano J, Rodriguez JR, DeFelipe J (2008) Gender differences in human cortical synaptic density. *Proc. Natl. Acad. Sci. USA* 105: 14615–14619. doi: 10.1073/pnas.0803652105 PMID: 18779570

67. Virgintino D, Monaghan P, Robertson D, Errede M, Bertossi M, et al (1997) An immunohistochemical and morphometric study on astrocytes and microvasculature in the human cerebral cortex. *Histochemical Journal* 29: 655–660. doi: 10.1023/A:1026448614647 PMID: 9413738

68. Arellano JI, Benavides-Piccione R, Yuste R, DeFelipe J (2007) Ultrastructure of dendritic spines: correlation between synaptic and spine morphologies. *Frontiers in Neuroscience* 1: 131–143. doi: 10.3389/neuro.01.1.1.010.2007 PMID: 18982124

69. Loewenstein Y, Kuras A, Rumpel S (2011) Multiplicative dynamics underlie the emergence of the log-normal distribution of spine sizes in the neocortex in vivo. *J. Neurosci.* 31: 9481–9488. doi: 10.1523/JNEUROSCI.6130-10.2011 PMID: 21715613

70. Song S, Sjöström PJ, Reigl M, Nelson SB, Chklovskii DB (2005) Highly nonrandom features of synaptic connectivity in local cortical circuits. *PLoS Biol.* 3: e68. doi: 10.1371/journal.pbio.0030068 PMID: 15737062

71. Peters A, Palay SL, Webster DF (1991) *The Fine Structure of the Nervous System*. Oxford: Oxford Univ. Press; 3rd edition.

72. Shepherd GM, Stepanyants A, Bureau I, Chklovskii D, Svoboda K (2005) Geometric and functional organization of cortical circuits. *Nat. Neurosci.* 8: 782–790. doi: 10.1038/nn1447 PMID: 15880111

73. Baron JC (2001) Perfusion thresholds in human cerebral ischemia: historical perspective and therapeutic implications. *Cerebrovasc. Dis* 11 (Suppl. 1): 2–8. doi: 10.1159/000049119 PMID: 11244194

74. Zhang S, Boyd J, Delaney K, Murphy TH (2005) Rapid reversible changes in dendritic spine structure in vivo gated by the degree of ischemia. *J. Neurosci.* 25: 5333–5338. doi: 10.1523/JNEUROSCI.1085-05.2005 PMID: 15930381

75. Kirov SA, Petrak LJ, Fiala JC, Harris KM (2004) Dendritic spines disappear with chilling but proliferate excessively upon rewarming of mature hippocampus. *Neuroscience* 127: 69–80. doi: 10.1016/j.neuroscience.2004.04.053 PMID: 15219670

76. Yasumatsu N, Matsuzaki M, Miyazaki T, Noguchi J, Kasai H (2008) Principles of long-term dynamics of dendritic spines. *J. Neurosci.* 28: 13592–13608. doi: 10.1523/JNEUROSCI.0603-08.2008 PMID: 19074033

77. Tieman SB, Moller S, Tieman DG, White JT (2004) The blood supply of the cat's visual cortex and its postnatal development. *Brain Res.* 998: 100–112. doi: 10.1016/j.brainres.2003.11.023 PMID: 14725973

78. Oberheim NA, Wang X, Goldman S, Nedergaard M (2006) Astrocytic complexity distinguishes the human brain. *Trends Neurosci.* 29: 547–553. doi: 10.1016/j.tins.2006.08.004 PMID: 16938356

79. Beardwood J, Halton JH, Hammersley JM (1959) The shortest path through many points. *Math. Proc. Cambridge* 55: 299–327. doi: 10.1017/S0305004100034095

80. Steele JM, Shepp LA, Eddy WF (1987) On the number of leaves of an Euclidean minimal spanning tree. *J. Appl. Probab.* 24: 809–826. doi: 10.2307/3214207

81. Ogata K, Kosaka T (2002) Structural and quantitative analysis of astrocytes in the mouse hippocampus. *Neuroscience* 113: 221–233. doi: 10.1016/S0306-4522(02)00041-6 PMID: 12123700

82. Oberheim NA, Takano T, Han X, He W, Lin JH, et al (2009) Uniquely hominid features of adult human astrocytes. *J. Neurosci.* 29: 3276–3287. doi: 10.1523/JNEUROSCI.4707-08.2009 PMID: 19279265

83. Boero JA, Ascher J, Arregui A, Rovainen C, Woolsey TA (1999) Increased brain capillaries in chronic hypoxia. *J. Appl. Physiol.* 86: 1211–1219. PMID: 10194205

84. Meier-Ruge W, Hunziker O, Schulz U, Tobler HJ, Schweizer A (1980) Stereological changes in the capillary network and nerve cells of the aging human brain. *Mechanisms of Ageing and Development* 14: 233–243. doi: 10.1016/0047-6374(80)90123-2 PMID: 7206813

85. DeFelipe J, Marco P, Fairen A, Jones EG (1997) Inhibitory synaptogenesis in mouse somatosensory cortex. *Cereb. Cortex* 7: 619–634. doi: 10.1093/cercor/7.7.619

86. Bell MA, Ball MJ (1985) Laminar variation in the microvascular architecture of normal human visual cortex (area 17). *Brain Res.* 335: 139–143. doi: 10.1016/0006-8993(85)90284-7 PMID: 4005537

87. O'Kusky J, Collonier M (1982) A laminar analysis of the number of neurons, glia, and synapses in the visual cortex (area 17) of adult macaque monkey. *J. Comp. Neurol.* 210: 278–290. doi: 10.1002/cne.902100307 PMID: 7142443

88. Huttenlocher PR, Dabholkar AS (1997) Regional differences in synaptogenesis in human cerebral cortex. *J. Comp. Neurol.* 387: 167–178. doi: 10.1002/(SICI)1096-9861(19971020)387:2%3C167::AID-CNE1%3E3.0.CO;2-Z PMID: 9336221

89. Erecinska M, Silver IA (1989) ATP and brain function. *J. Cereb. Blood Flow Metab*. 9: 2–19. doi: 10.1038/jcbfm.1989.2 PMID: 2642915

90. Press WH, Teukolsky SA, Vetterling WT, Flannery BP (1992) *Numerical Recipes in Fortran*. Cambridge: Cambridge Univ. Press.

91. Spencer NH (2014) *Essentials of Multivariate Data Analysis*. Boca Raton: CRC Press.